의학박사 학위논문

Radiation-induced change of PD-1/PD-L1 immune checkpoint in mouse and human colorectal cancer models

대장직장암 모델 기반 방사선 조사 후
PD-1/PD-L1 면역 관문의 변화에 관한 연구

2018년 2월

서울대학교 대학원
임상의과학과 방사선종양학 전공
임 유 진

ABSTRACT

Radiation-induced change of PD-1/ PD-L1 immune checkpoint in mouse and human colorectal cancer models

Yu Jin Lim

Clinical Medical Sciences (Radiation Oncology)

The Graduate School

Seoul National University

Introduction: Recent progress in immunotherapy has introduced programmed death-1 (PD-1)/ programmed death-ligand 1 (PD-L1) blockade as a novel target to eradicate tumors, but its use has been mainly confined to recurrent or metastatic settings. Radiotherapy (RT), a major part of anti-cancer treatment, directly kills tumor cells, and subsequent anti-tumor immune responses are up-regulated. However, immunologic impacts of RT on PD-1/PD-L1 immune checkpoint activity has not been much investigated. This study evaluated RT-induced alterations of the PD-1/PD-L1 checkpoint molecules based on a murine colon carcinoma and human rectal cancer treated with preoperative chemoradiotherapy (CRT).

Methods: CT26 colon carcinoma cell line was subcutaneously inoculated on the right hind leg of BALB/c mice. Based on tumor growth curves after irradiation of 15 Gy x 1 fx or 5 Gy x 3 fx, mouse tumors were surgically resected on 4 different time points: "Pre-RT", non-irradiated status just prior to initiation of RT; "Early", the early phase of RT response; "Nadir", representing minimal tumor volume; and "Regrowth", with regrown tumors after RT. Defining the Day 1 as an initiation of RT, tumor tissues were obtained on Day 1, 6, 12, and 22, and Day 1, 6, 10, and 20, with single ablative and fractionated dose regimen, respectively. PD-L1 expression on tumor cells, PD-1 expression on tumor-infiltrating $CD4^+$ and $CD8^+$ T cells, and proportions of tumor-infiltrating $CD4^+$ and $CD8^+$ T cell populations were estimated using flow cytometry analysis. Considering human data, we conducted paired analysis using pre-CRT biopsies and the corresponding post-CRT resected tissues of 123 rectal cancer patients undergoing preoperative CRT followed by surgery between 2005 and 2012. Immunohistochemistry of PD-L1, PD-1, and CD8 was analyzed along with other clinicopathologic features and survival outcomes.

Results: PD-L1 expression on mouse tumor cells surged within a few days after completion of RT, followed by abrupt decreases on the "Nadir" and "Regrowth" phases ($P < .001$ and equal to .002 for single ablative and fractionated RT, respectively). PD-1-positivity (%) on $CD4^+$ T cells was not significantly different according to different time points ($P = .656$ and .223 for single ablative and fractionated RT, respectively). On the contrary, PD-1-

positive proportions (%) in $CD8^+$ T cells sharply increased, and the high-level was sustained until the "Regrowth" phase ($P < .001$ for all paired comparisons between "Pre-RT" and others). During RT response of "Early" and "Nadir" time points, $CD4^+$ T cells decreased, but $CD8^+$ T cells increased. The alterations were reversed at "Regrowth" phase, with increasing and decreasing again in $CD4^+$ and $CD8^+$ T cell populations, respectively ($P < .001$ all paired comparisons between "Pre-RT" and others).

In the immunohistochemistry of rectal cancer, PD-L1 expression levels and density of $CD8^+$ tumor-infiltrating lymphocytes (TILs) increased after CRT ($P < .001$ for both). Considering PD-1 expression, its pre-CRT intensity was scanty, but markedly increased after CRT. With cutoffs using each median value, sustained higher expression of PD-L1 at pre- and post-CRT (high-to-high) was associated with less increase in the density of $CD8^+$ TILs ($P = .020$). Patients with sustained high-to-high PD-L1 expression had poorer overall survival (OS) and disease-free interval (DFI) in univariate Kaplan-Meier analysis ($P = .018$ and .029, respectively), with inferior DFI in low-to-low density $CD8^+$ TILs ($P = .010$). In multivariate analysis, two subgroups with high baseline PD-L1 expression level showed worse OS, but the highest risk was observed with the high-to-high alteration (hazard ratio [HR] 8.34, 95% confidence interval [CI] 1.85–37.53 and HR 11.03, 95% CI 2.33–52.29 for high-to-low and high-to-high, respectively).

Conclusions: This study verified radiation-induced immunologic shift toward increases of the PD-1/PD-L1 checkpoint activity and density of $CD8^+$ TILs.

However, the change was maximal at the early phase of RT response, which highlights the need of concurrent combinatory strategy of PD-L1 blockade and RT. The alteration profiles of checkpoint-related molecules identified the subset of patients with poor prognosis, suggesting potential candidates who can benefit from combining checkpoint inhibitors.

Keywords: PD-L1, PD-1, CD8, radiotherapy, mouse tumor model, rectal cancer, chemoradiotherapy

Student number: 2014-30918

CONTENTS

LIST OF TABLES AND FIGURES

LIST OF ABBREVIATION

PD-1, programmed death-1

PD-L1, programmed death-ligand 1

MSI, microsatellite instability

MSS, microsatellite-stable

RT, radiotherapy

CRT, chemoradiotherapy

IHC, immunohistochemistry

BED, biologically effective dose

HBSS, Hank's Balanced Salt Solution

IRB, Institutional Review Board

MSI-H, microsatellite instability-high

MSI-L, microsatellite instability-low

TILs, tumor-infiltrating lymphocytes

SD, standard deviation

OS, overall survival

DFI, disease-free interval

LRFI, locoregional relapse-free interval

DMFI, distant metastasis-free interval

MFI, median fluorescence intensity

HR, hazard ratio

CI, confidence interval

INTRODUCTION

Cancer immunotherapy has been one of the major anti-cancer modalities to suppress or eradicate tumors. In the function of T cell-mediated anti-cancer immunity, regulation of co-stimulatory or inhibitory signals is an important underlying mechanism (1). Immune checkpoints are molecules that either up-regulate or down-regulate cascade immune reactions, which has been increasingly considered as a novel target for cancer treatment (2).

Programmed death-1 (PD-1) (known as CD279) is a cell surface receptor expressed on T cells and pro-B cells (3). Programmed death-ligand 1 (PD-L1) (known as B7-H1 or CD274) is its main ligand widely expressed on antigen-presenting cells, normal epithelial or endothelial tissues, and tumor cells (3). PD-1/PD-L1 is one of the prominent immune checkpoints, well-known as inhibitory mechanisms of immune responses (4). Their molecular interaction under pro-inflammatory conditions induces co-inhibitory signal of immune responses with down-regulation of cytokine levels and effector T cells (5). Although the PD-1/PD-L1 immune checkpoint plays a physiologic function in down-regulating harmful inflammation reactions, the inhibitory effect leads to immune evasion and further tumor progression in the tumor microenvironment (6). The advent of PD-1/PD-L1-inhibiting strategy has highlighted the critical role of anti-tumor immunity in a variety of human cancers.

Colorectal cancer is the third most common cancer worldwide (7). Despite

technical advances and development of targeted therapies, this malignancy is the second to third leading cause of cancer-related deaths (7). Post-treatment failure with metastatic tumor spread still needs to be overcome (8). Although the use of the PD-1/PD-L1 checkpoint inhibitors has been considered a possible anti-cancer treatment option, previous clinical trials could not demonstrate a clear benefit in colorectal cancer (9). At baseline for colorectal cancer, PD-L1 expression in tumor cells is not often directly linked to their response to the checkpoint blockade therapy, whereas the checkpoint inhibitor is more effective in tumors of microsatellite instability (MSI) status, rather than microsatellite-stable (MSS) status (10, 11). Therefore, determining an optimal indication of the immunotherapeutic approach has been of interest to treatment of colorectal cancer.

With regard to the immunologic equilibrium, it has been known that cytotoxic therapies, such as chemotherapy, radiotherapy (RT), and chemoradiotherapy (CRT), develop a pro-inflammatory tumor microenvironment, releasing danger signals and allowing the activation of tumor-specific adaptive immunity (12, 13). In addition to previous investigations demonstrating the effect of RT as an immune adjuvant (14-17), recent preliminary results have supported combining PD-1/PD-L1 inhibitors with chemotherapy or CRT (18-20). To expand the discussion more in clinics, the potential for shifting the PD-1/PD-L1 activity through cytotoxic anti-cancer treatment needs to be explored.

In this study, we hypothesized that: 1) PD-1/PD-L1 expressions undergo alterations through the time course after RT based on syngeneic murine tumor

model; 2) Pre- and post-treatment change of PD-1/PD-L1 status of human cancer tissues is in accordance with that of mouse tumors; 3) PD-1/PD-L1 expression levels before and/or after treatment are associated with patients' prognosis. Since tumor tissues are not routinely obtained after RT in clinics, CT26 murine colon carcinoma model was used for post-RT consecutive monitoring of the checkpoint activity. To validate the alteration tendency regarding its prognostic associations in human cancer, we performed a paired comparison analysis using immunohistochemistry (IHC) of initial biopsies and post-CRT surgical tissues of rectal cancer undergoing preoperative CRT followed by surgery. Our results would provide knowledge for an optimal schedule and indication of combining strategy of conventional cytotoxic therapy and immune checkpoint inhibitors.

MATERIALS AND METHODS

1. Cell line and animals

CT26 cell line, a murine colon carcinoma of BALB/c mouse, was purchased from American Type Culture Collection. The cells were maintained in Roswell Park Memorial Institute medium (Welgene, Gyeongsan-si, Gyeongsangbuk-do, Korea) supplemented with 10% fetal bovine serum (Gibco, Grand Island, NY, USA) and antibiotic-antimycotic (100x) (Gibco, Grand Island, NY, USA), and grown in an incubator with humidified atmosphere of 95% air and 5% CO_2 at 37.5 ℃.

Male 6-week old BALB/c mice were used in this study. The animal experiment was approved by the Institutional Animal Care and Use Committee of Seoul National University Hospital (approval number: 15-0199-C1A0). All experimental procedures were conducted under the regulations and standards of the institution.

2. Preliminary experiments

To determine details of mouse tumor model, such as tumor cell counts, inoculation methods, radiation dose, energy, and initial tumor volume at the start of irradiation, other prior CT26 murine model-based protocols were considered (17, 21). In the pilot study, 2×10^5 CT26 cells were subcutaneously inoculated at right lower hind leg of mice. Mouse tumors were irradiated with 6-MV X-ray photon energy once daily using a linear accelerator (Varian Medical systems, Palo Alto, CA). A custom-made acrylic device was used to immobilize the body and leg tumors (Figure 1).

Tumor size was measured every other day using a vernier caliper without treatment information. Individual tumor volume was calculated with the formula of 1/2 x length x width^2 (mm^3)

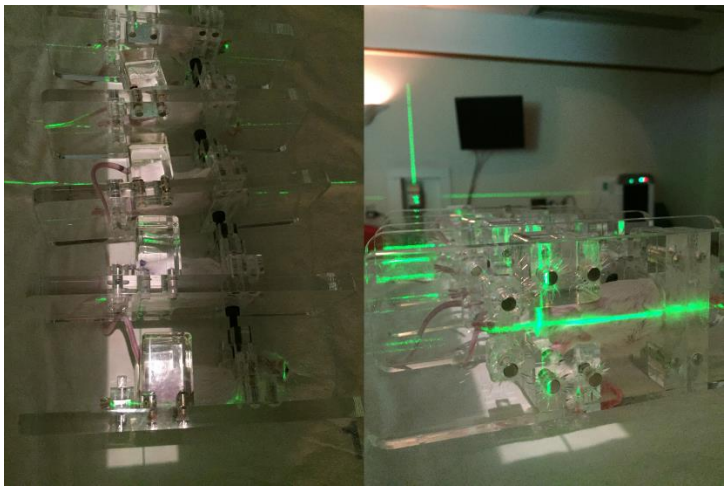

Figure 1. Immobilization and irradiation of mouse tumors

Regarding that dose regimens used in the two reference studies are converted to biologically effective dose (BED) of 7.5−8 Gy_{10}, our pilot study explored single and fractionated radiation dose schemes: 7.5 Gy x 1 fx, 2.5 Gy x 3 fx, 15 Gy x 1 fx, and 5 Gy x 3 fx. Tumor growth curves of control (no radiation) and the above 4 experimental groups were compared (Figure 2). To evaluate immunologic effects of radiation-induced tumor cell killing, 15 Gy x 1 fx and 5 Gy x 3 fx, showing definite increasing, decreasing, and regrowth patterns after irradiation, were selected.

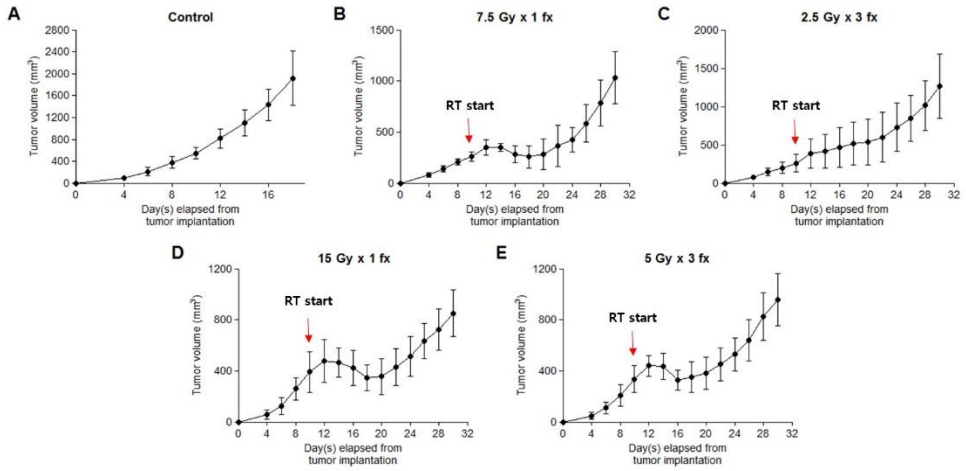

Figure 2. Preliminary experiments for tumor growth curves after irradiation: (A) Control (no RT), (B) 7.5 Gy x 1 fx, (C) 2.5 Gy x 3 fx, (D) 15 Gy x 1 fx, (E) 5 Gy x 3 fx. *Red arrows* indicate the start of irradiation. Representative data (mean ± standard deviation) (mm^3) of 5 mice per each RT dose regimen.

From comprehensive review of the preliminary results, other experimental protocols were determined: tumor cell count of 5 x 10^5, right lower hind leg as the subcutaneous injection site with a fixation device, and initial tumor volume at least 200 mm^3. The same researchers (Y.J.L. and S.R.J.) consistently performed the tumor inoculation and irradiation to obtain reproducible results.

3. Mouse tumor model

Based on tumor growth curves with irradiation, four different time points for resection of tumor tissues were determined for each of single ablative and

fractionated dose regimen: “Pre-RT”, non-irradiated status just prior to initiation of RT; “Early”, the early phase of RT response; “Nadir”, representing minimal tumor volume; and “Regrowth”, with regrown tumors after RT (Figure 3). Defining the day 1 as an initiation of RT with 15 Gy x 1 fx or 5 Gy x 3 fx, the “Early”, “Nadir”, and “Regrowth” phases were in accordance with day 6, 12, and 22, or day 6, 10, and 20, respectively. Every four mice were sacrificed at each time point for tumor resection, and expressions of the immune checkpoint-related molecules were evaluated.

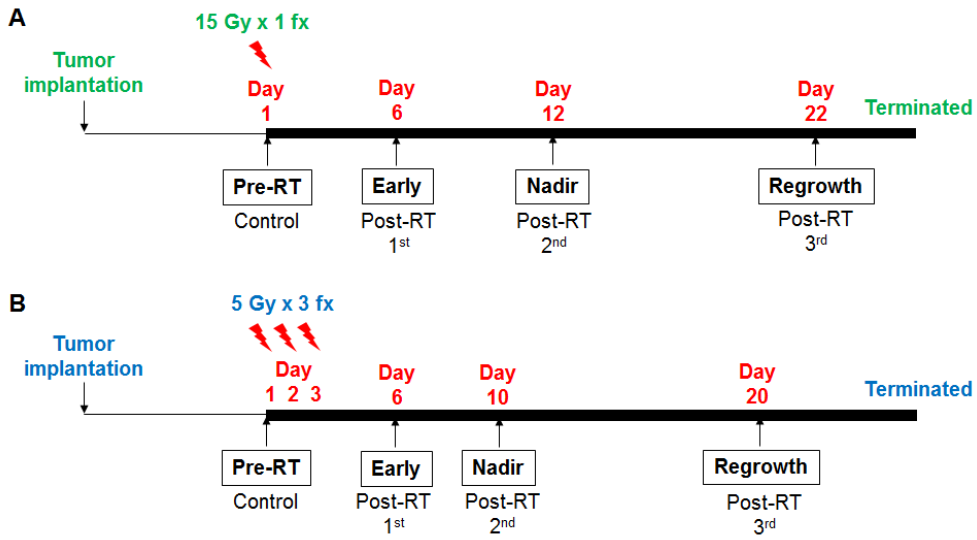

Figure 3. Four different time points for evaluation of PD-1/PD-L1 immune checkpoint activity on mouse tumor tissues. (A) Single ablative dose (15 Gy x 1 fx) and (B) fractionated (5 Gy x 3 fx) irradiation: “Pre-RT”, non-irradiated status just prior to initiation of RT; “Early”, the early phase of RT response; “Nadir”,

representing minimal tumor volume; and “Regrowth”, with regrown tumors after RT.

4. Single cell suspension of mouse tumors

Tumor tissues were cut up into small pieces and minced using scalpels. For digestion, 10x triple enzyme stock solution, consisting of 10 mg/ml collagenase IV, 200 mg/ml DNase I, 1 mg/ml hyaluronidase, and Hank’s Balanced Salt Solution (HBSS) (all Sigma-Aldrich, St. Louis, MO, USA), was added. The sample was incubated under 37℃ for 30 min, and passed through 70 μm nylon mesh cell strainer (Corning, Corning, NY, USA). After repeated washing in HBSS, cells were resuspended with plating media.

5. Flow cytometry analysis

Prepared cells were initially blocked with anti-FcR (BD Biosciences, San Jose, CA, USA), and then stained with antibodies against CD45, CD3, CD4, CD8, PD-1 (BioLegend, San Diego, CA, USA), and PD-L1 (BD Biosciences unless otherwise stated). Live cells were gated using a fixable viability stain reagent (BD Biosciences, San Jose, CA, USA). Phenotypes of tumor cells and lymphocytes were evaluated. Figure 4 and 5 represent gating strategies to discriminate $CD45^{+}CD3^{+}$ and $CD45^{-}$ cells, respectively.

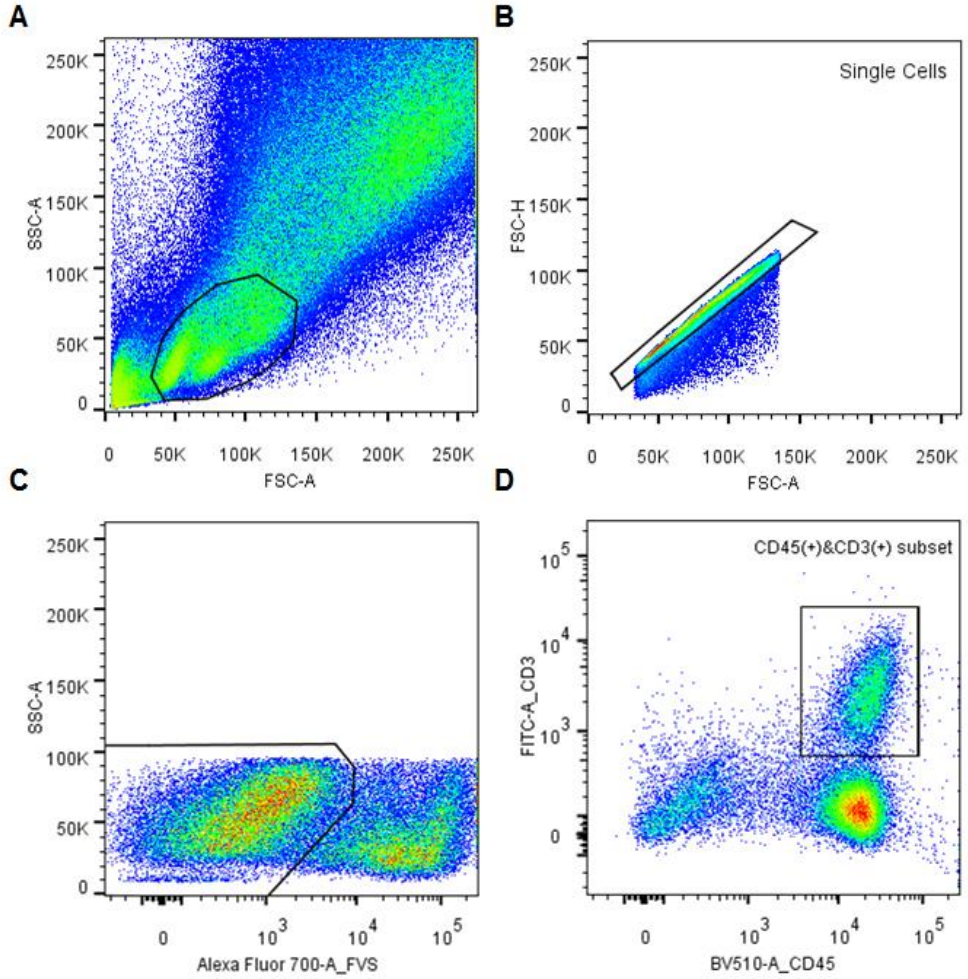

Figure 4. Gating method for evaluation of PD-1 expression in subsets of $CD45^{+}CD3^{+}$ cells. (A, B) Selection based on size and granularity information, (C) gating for viable cells based on vital dye exclusion pattern, and (D) discrimination of $CD45^{+}$ and $CD3^{+}$ cell population.

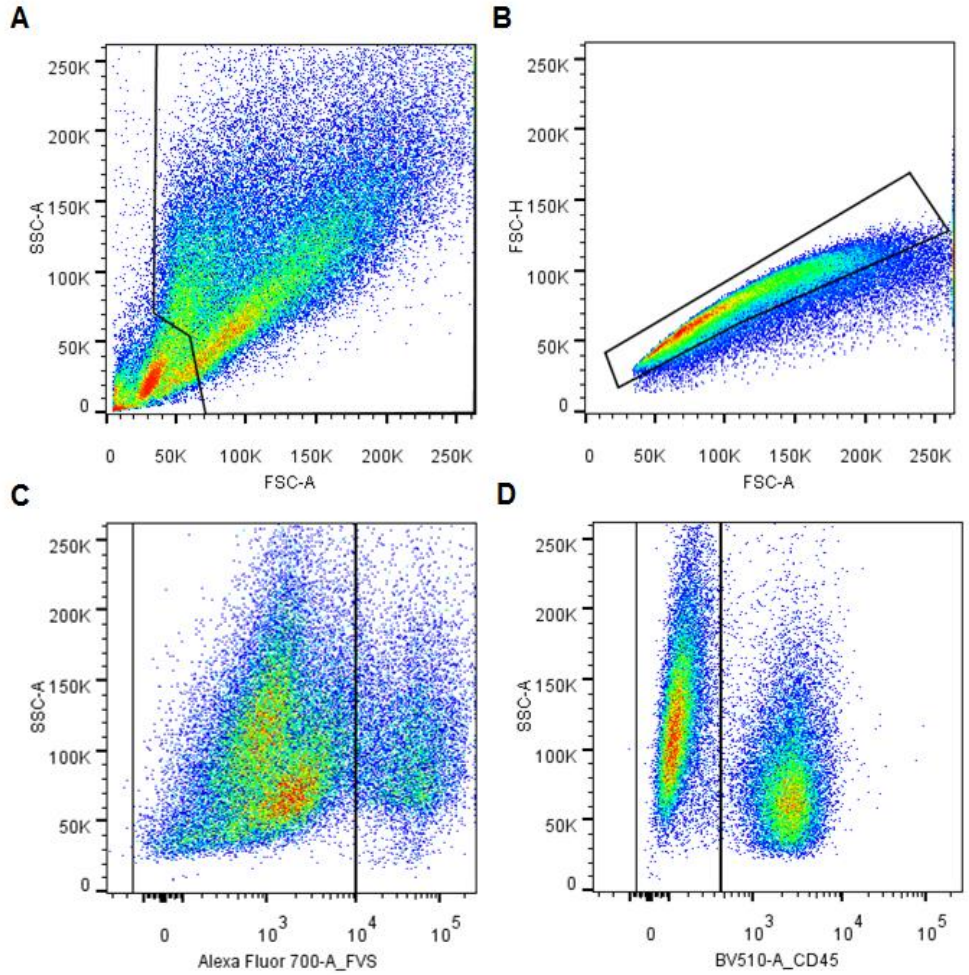

Figure 5. Gating method for evaluation of PD-L1 expression on tumor cells. (A, B) Selection based on size and granularity information, (C) gating for viable cells based on vital dye exclusion pattern, and (D) discrimination of $CD45^-$ cell population.

6. Patient population

Rectal cancer patients undergoing preoperative CRT plus total mesorectal excision between 2005 and 2012 at our hospital were reviewed, and a total of 123 patients were finally analyzed. The eligibility criteria included: 1) both biopsy and postsurgical tumor tissues obtained; 2) clinicopathologic information fully available; 3) initial cM0 stage; 4) preoperative CRT with conventional fractionation; and 5) completion of planned course of CRT plus total mesorectal excision. This study was approved by the Institutional Review Board (IRB) of our institution (IRB No. 1503-039-654). The Declaration of Helsinki principles were followed throughout the present analysis.

Clinical and pathologic tumor stages were classified according to the 7th edition of the American Joint Committee on Cancer staging system. The pathologic regression grade was based on the Dworak system, from 0 of no regression to 4 of complete pathological regression (22). The MSI analysis was performed using fluorescent multiplex polymerase chain reaction with the five markers recommended by the National Cancer Institute workshop: BAT-25, BAT-26, D5S346, D17S250, and D2S123. Using DNA analysis, samples with two or more of the markers were considered as MSI-high (MSI-H). The presence of one marker corresponded to MSI-low (MSI-L), and the MSS status was diagnosed when all of the markers represented stability.

7. Treatment of patients

Patients with rectal adenocarcinoma of clinically T3–4 and/or node-positive status were referred for preoperative CRT. With a daily fraction size of 1.8 Gy, the median total radiation dose was 50.4 Gy (range, 50.4–55.8). The concurrent chemotherapy regimen included intravenous 5-fluorouracil (500 mg/m^2 for 3 days during the first and fifth week of radiation) and oral capecitabine (1,650 mg/m^2 daily during the course of radiation). Following the preoperative CRT, the patients underwent total mesorectal excision, with the median time interval of 52 days (range, 38–82). Most patients (92%) received postoperative maintenance chemotherapy.

8. Immunohistochemistry

Tissue specimens from initial biopsies (pre-CRT) and total mesorectal excision (post-CRT) were retrieved from the pathology archive of our institution. The cases were reviewed and histologically confirmed as adenocarcinoma. A tissue microarray was made with 4-mm cores from formalin-fixed paraffin-embedded tissue blocks, with two representative cores of invasive front of tumors for each case. For the immunohistochemical staining of PD-L1, PD-1, and CD8, rabbit anti-PD-L1 antibody Q9NZQ7 (Abcam, Cambridge, MA, USA; 1:700), mouse anti-PD-1 antibody NAT105 (Cell Marque, Rocklin, CA, USA; 1:100), and rabbit anti-CD8 antibody SP57 (Roche, Indianapolis, IN, USA; ready-to-use) were used. For the immunohistochemical staining, Ventana BenchMark XT autostainer (Ventana Medical Systems, Tucson, AZ, USA) was used. Human placenta and tonsil tissues

were used for positive control of anti-PD-L1, and PD-1 or CD8 staining, respectively (Figure 6).

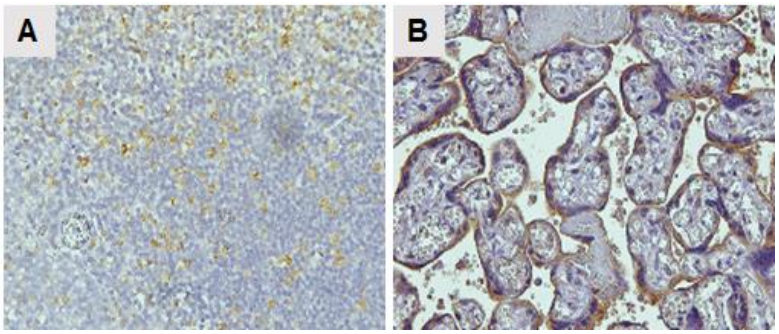

Figure 6. Positive control of immunohistochemistry. Slide views of human (A) tonsil and (B) placenta tissues stained with anti-PD-1 and PD-L1 antibody, respectively (x200).

9. Pathologic evaluation

PD-L1 expression in tumor tissues was assessed semi-quantitatively on a 0–3 scale (0, no; 1, weak; 2, moderate; and 3, strong expression). H-score was calculated using the formula, the representative staining intensity of each case × the percentage of expressed tumor cells. Although the PD-L1 molecule is expressed on both tumor and tumor-infiltrating immune cells, such as macrophages and lymphocytes, the expression on lymphocytes was not sufficiently observed in our paraffin-embedded tissues. Then, we designed our study focusing on the altered PD-L1 expression based on membranous staining of tumor cells.

The CD8-stained slides were scanned using an AperioScanScope (Aperio Technologies, Vista, CA, USA). Based on the Aperio nuclear IHC algorithms of spectral differentiation between brown (positive) and blue (counter) staining, total positivity percentage was scored as 1+ through 3+ for each case. The density of $CD8^+$ tumor-infiltrating lymphocytes (TILs) was automatically enumerated, which was defined as the total number of 1+ to 3+ cells divided by the total area (mm^2). Two pathologists (J.K. and S.K.) reviewed the staining results without any clinical information of each patient.

10. Statistical analysis

Tumor growth curve data of CT26 mouse tumor model were presented as mean ± standard deviation (SD) of absolute tumor volume (mm^3). To evaluate differential expression of immunologic markers among the four kinds of time points, one-way analysis of variance method was used. The relationships between baseline characteristics of rectal cancer patients and PD-L1 expression on tumor cells were evaluated by the Pearson's chi-square or Fisher's exact test, and the Wilcoxon signed-rank test was used for the analysis of $CD8^+$ TILs. In survival analysis, the primary outcome of interest was overall survival (OS), which was defined as the time period between the start date of CRT and overall death events. Disease-free interval (DFI), locoregional relapse-free interval (LRFI), and distant metastasis-free interval (DMFI) were estimated based on the overall, locoregional, and distant metastatic recurrence events, respectively. Kaplan-Meier analysis with a log-rank

test and a Cox proportional hazards model were used to evaluate prognostic factors. Statistically significant factors indicating *P*-values less than 0.05 were considered statistically significant. All analyses were conducted with SPSS 22 (IBM, Armonk, NT, USA).

RESULTS

Tumor growth curve after irradiation

Figure 7 represents the change of absolute tumor volume before and after irradiation using the CT26 murine tumor model. When tumors were irradiated with a single ablative dose of 15 Gy x 1 fx, the tumor growth delay comprising of descending and regrowth change was observed. The consecutive phase of RT response with 5 Gy x 3 fx was also characteristic, but tumor regrowth appeared earlier than with single ablative dose regimen.

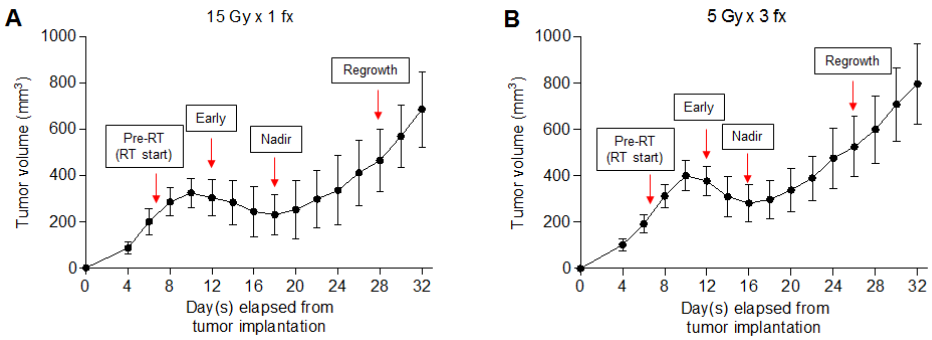

Figure 7. Change of CT26 tumor volume with irradiation. Black dot symbols and error bars indicate mean and SD values from 5 mice per each dose regimen, respectively, with (A) single ablative (15 Gy x 1 fx) and (B) fractionated (5 Gy x 3 fx) RT. *Red arrows* indicate the time points of tumor resection. Experiments were repeated twice, and the representative data are shown here.

PD-L1 expressions on tumor cells

Compared to baseline status, irradiated tumors at "Early" phase showed a sharp increase of PD-L1 expression on tumor cells. The mean ± SD values of median fluorescence intensity (MFI) at "Pre-RT" and "Early" were 1188.8 ± 549.2 and 4923.0 ± 633.6, and 969.5 ± 187.2 and 4604.8 ± 2021.8 with single ablative and fractionated RT, respectively. However, the intensity abruptly decreased again through the "Nadir" and "Regrowth" time points, with 1525.5 ± 211.4 and 845.5 ± 253.9, and 1859.0 ±326.4 and 1584.0 ± 282.1, respectively. All paired comparisons between the maximum at "Early" phase and the other time points were statistically significant (Figure 8). Representative histograms are presented in Figure 9.

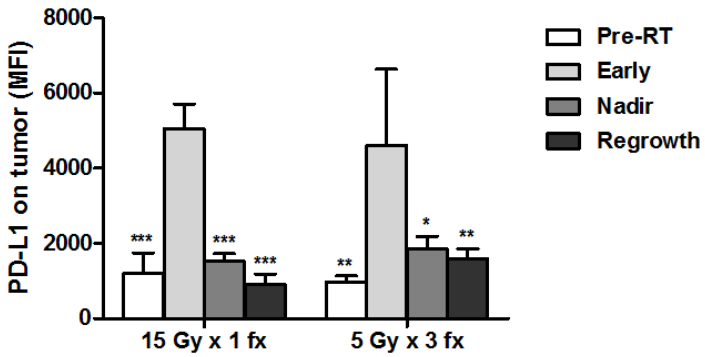

Figure 8. Alterations in median fluorescence intensity of PD-L1 on tumor cells before and after RT. $^{*}P < .05$, $^{**}P < .01$, and $^{***}P < .001$ in comparison with the "Early" status. Mean ± SD values are represented from 4 mice per each time point

after 15 Gy x 1 fx and 5 Gy x 3 fx, respectively. Experiments were repeated twice, and the representative data are shown here.

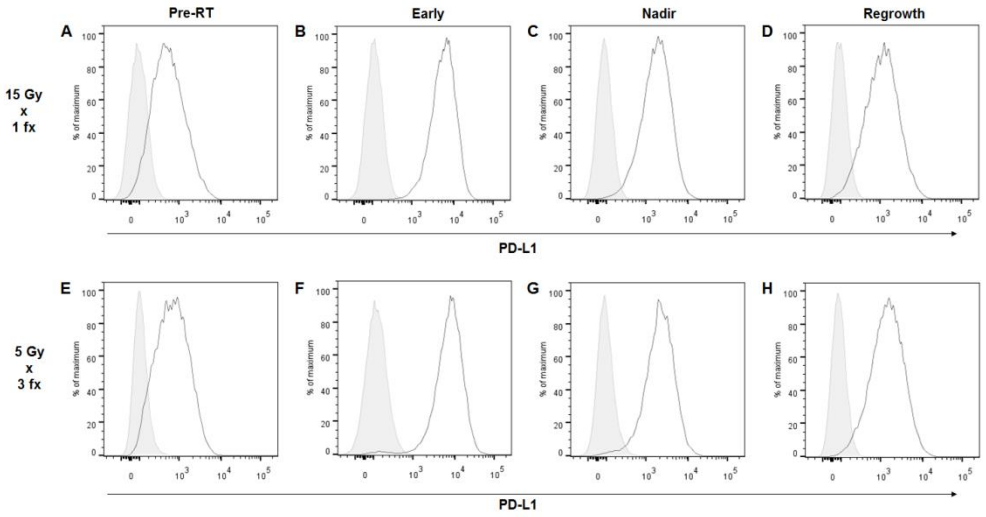

Figure 9. PD-L1 expression on tumor cells according to different time points before and after RT. Representative results of isotype control (*grey shadow*) and PD-L1 (*black solid line*) with (A−D) single ablative and (E−H) fractionated RT are presented, respectively.

PD-1 expression on $CD4^+$ and $CD8^+$ T cells

Figure 10 represents comparisons of PD-1 expression on $CD4^+$ and $CD8^+$ T cells at the different time points. The mean ± SD values of $PD\text{-}1^+$ proportions (%) relative to $CD4^+$ T cell population at "Pre-RT", "Early", "Nadir", and "Regrowth" phase were 57.4 ± 12.6, 63.7 ± 6.4, 57.1 ± 7.5, and 60.0 ± 4.3, and 55.1 ± 15.3, 67.4 ±

11.9, 70.6 ± 9.5, and 57.2 ± 8.7 with single ablative and fractionated RT dose, respectively (P = .656 and .223, respectively). Considering the expression level of PD-1 on $CD8^+$ T cells, the proportions of positive cells increased much sharply, and the high-level was sustained until the "Regrowth" phase. The mean ± SD values of PD-1-positivity (%) among the $CD8^+$ T cells at the aforementioned 4 time points were 23.4 ± 8.9, 95.5 ± 0.7, 93.8 ± 6.2, and 88.0 ± 10.0, and 35.8 ± 7.2, 96.4 ± 2.8, 96.8 ± 2.0, and 88.3 ± 6.2, with single ablative and fractionated RT dose, respectively (P < .001 for both). Figure 11 shows representative histogram data of PD-1 expression on $CD4^+$ and $CD8^+$ T cells.

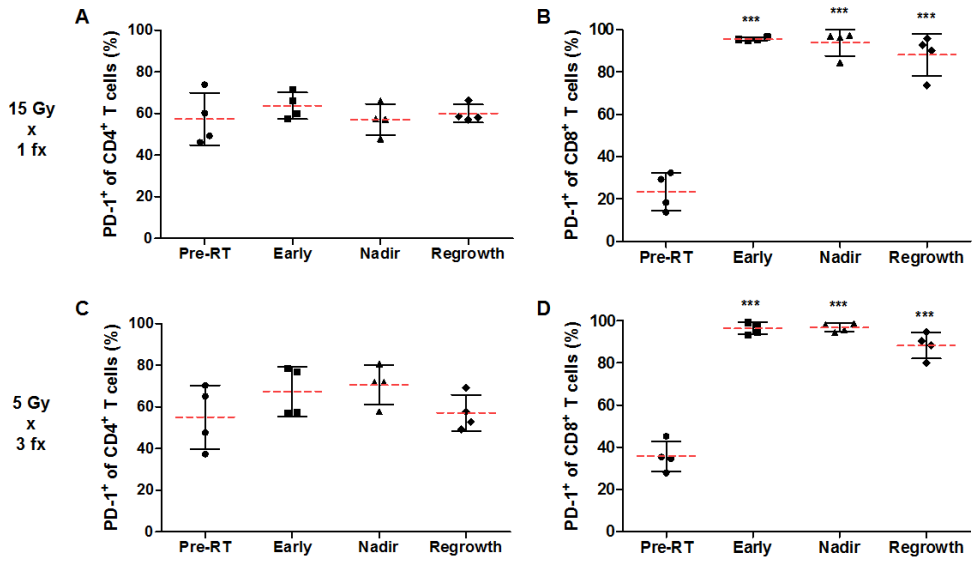

Figure 10. PD-1 expression on (A, C) $CD4^+$ and (B, D) $CD8^+$ T cells with single ablative (*upper panel*) and fractionated RT (*lower panel*). Proportions of PD-1-positive cells relative to $CD4^+$ and $CD8^+$ subsets are represented as mean (*red*

dotted line) ± SD (*error bars of black solid line*) values from 4 mice per each time point after 15 Gy x 1 fx and 5 Gy x 3 fx, respectively. Experiments were repeated twice, and the representative data are shown here.

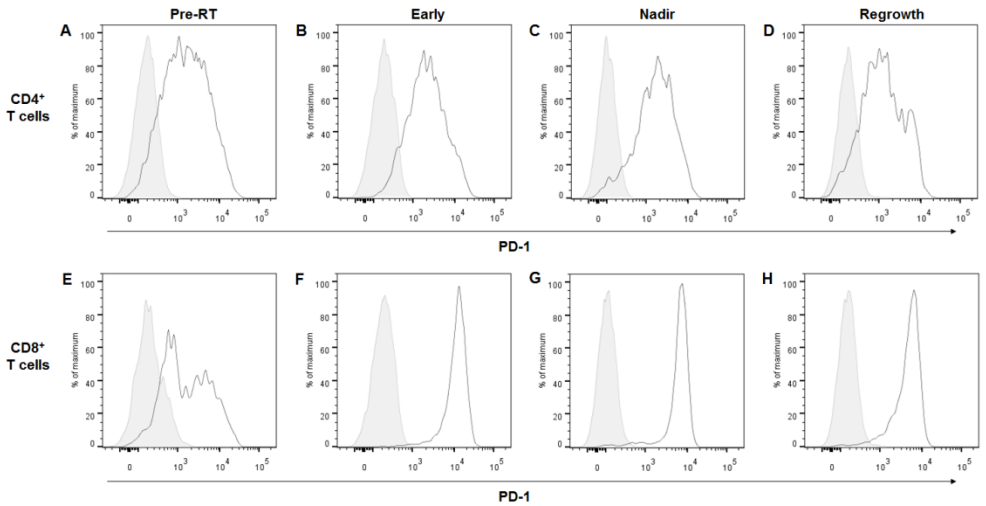

Figure 11. Representative histograms of PD-1 expression on (A−D) $CD4^+$ and (E−H) $CD8^+$ T cells according to different time points after RT. Results of isotype control (*grey shadow*) and PD-1 (*solid line*) are presented.

Proportions of $CD4^+$ and $CD8^+$ T cell subsets

$CD4^+$ subset decreased after RT, and then increased again at "Regrowth" phase. The $CD4^+$ proportions (%) among the T cells at "Pre-RT", "Early", "Nadir", and "Regrowth" were 76.7 ± 2.5, 18.0 ± 6.0, 21.7 ± 11.5, and 42.4 ± 5.5, and 89.3 ± 6.9, 27.2 ± 17.6, 20.4 ± 6.7, and 39.3 ± 7.9 with single ablative and fractionated RT, respectively (mean ± SD values) ($P < .001$ for all paired comparisons between the

"Pre-RT" and others) (Figure 12). On the contrary, the $CD8^+$ T cell population sharply increased after RT, and subsequently decreased at "Regrowth" phase. The mean ± SD values of CD8-positivity (%) relative to T cell population at the aforementioned 4 time points were 8.3 ± 2.5, 66.1 ± 7.6, 67.5 ± 10.8, and 47.2 ± 5.8, and 8.8 ± 4.4, 71.9 ± 17.0, 75.6 ± 9.1, and 53.1 ± 15.9 with single ablative and fractionated RT, respectively ($P < .001$ for all paired comparisons between the "Pre-RT" and others). Figure 13 shows representative contour dot plots of $CD4^+$ and $CD8^+$ T cell populations according to different time points.

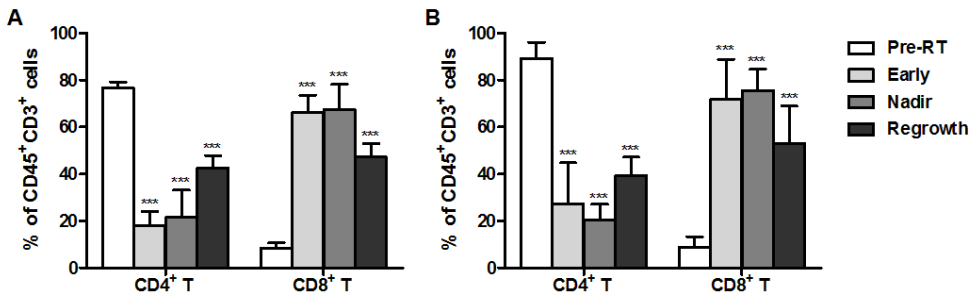

Figure 12. Altered proportions of $CD4^+$ and $CD8^+$ T cell subsets relative to $CD45^+CD3^+$ cells after irradiation. (A) Single ablative and (B) fractionated dose regimen. Mean ± SD values are represented from 4 mice per each time point after 15 Gy x 1 fx and 5 Gy x 3 fx, respectively. $^{***}P < .001$ in comparison with the "Pre-RT" status. Experiments were repeated twice, and the representative data are shown here.

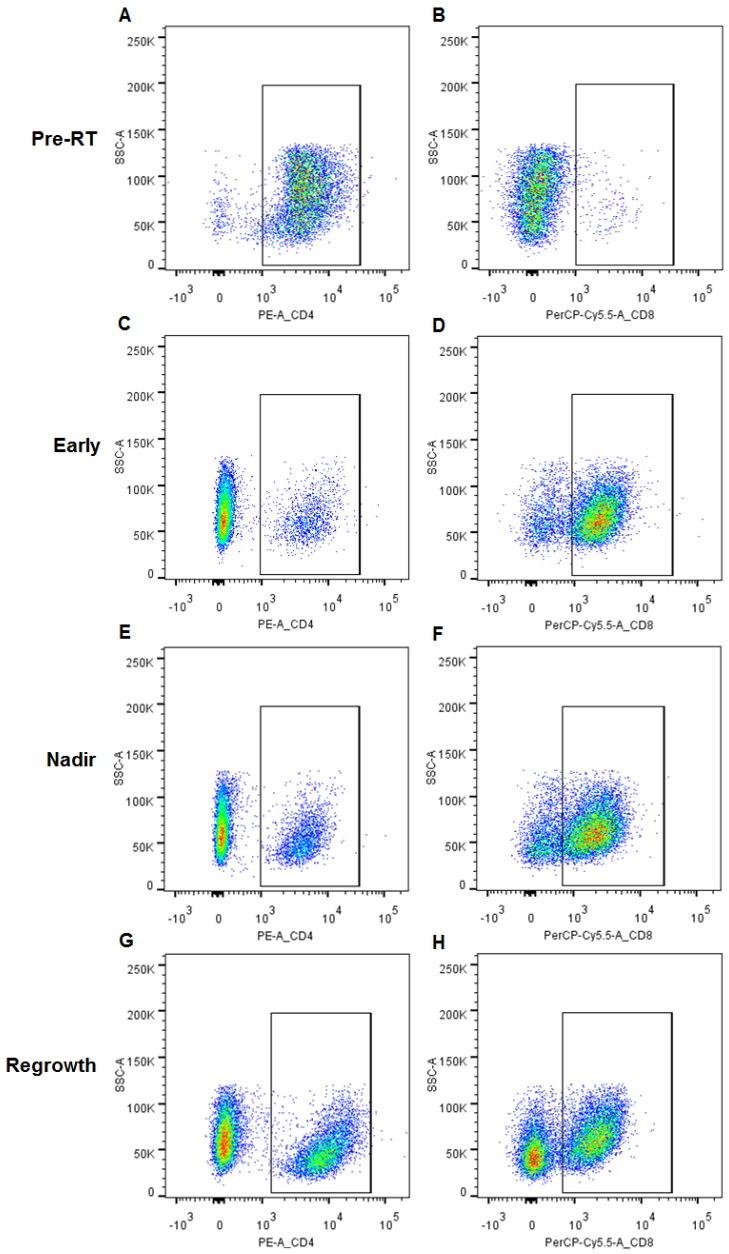

Figure 13. Change of $CD4^+$ (*left panel*) and $CD8^+$ (*right panel*) T cell populations according to different time points: (A, B) "Pre-RT", (C, D) "Early", (E, F) "Nadir", and (G, H) "Regrowth", respectively.

Clinicopathologic characteristics of rectal cancer patients

Baseline patient and tumor-related characteristics are summarized in Table 1. The median age was 62 years (range, 29–86), and 86 (70%) patients were men. Most patients (86%) had cT3 tumors, and 18 (15%), 41 (33%), and 64 (52%) patients were diagnosed as pT1, pT2, and pT3 in surgical specimens, respectively. Clinically node-positive disease was diagnosed in 106 (86%) patients, and 31 (25%) patients had pathologically positive nodal status. Pathologic down-staging of T and N was observed in 63 (51%) and 81 (66%) patients, respectively. Based on the Dworak's system (21), pathologic tumor regression of grade 2 or higher was reported in 62 (51%) patients. The MSI-L or MSI-H status was observed in 9 (7%) patients. Concurrent 5-fluorouracil and capecitabine were administered to 90 (73%) and 33 (27%) patients, respectively.

Table 1. Characteristics of rectal cancer patients

Variables	No. of patients (%)
Age (years)	
Median (range)	62 (29–86)
< 62	60 (49)
≥ 62	63 (51)
Sex	
Male	86 (70)
Female	37 (30)
Tumor location from anal verge*	
< 6cm	71 (58)
≥ 6cm	52 (42)
Tumor grade (biopsy)	
Well differentiated	18 (15)
Moderately/Poorly differentiated	105 (85)
cT stage	
T2	7 (6)
T3	106 (86)
T4	10 (8)
cN stage	
N0	17 (14)
N1	91 (74)
N2	15 (12)
Tumor grade (resected)	
Well differentiated	9 (7)
Moderately/Poorly differentiated	114 (93)
pT stage	
T1	18 (15)
T2	41 (33)
T3	64 (52)
pN stage	
N0	92 (75)
N1	26 (21)
N2	5 (4)
Downstage of T	
Yes	63 (51)
No	60 (49)
Downstage of N	
Yes	81 (66)
No	25 (20)
cN0	17 (14)
Dworak regression grade	

0	5 (4)
1	53 (43)
2	49 (40)
3	13 (11)
Not reported	3 (2)
Lymphatic invasion	
No	103 (84)
Yes	18 (14)
Unknown	2 (2)
Vascular invasion	
No	116 (94)
Yes	5 (4)
Unknown	2 (2)
Perineural invasion	
No	107 (87)
Yes	14 (11)
Unknown	2 (2)
Microsatellite instability (MSI)	
Microsatellite-stable	91 (74)
MSI-low	4 (3)
MSI-high	5 (4)
Unknown	23 (19)
Concurrent chemotherapy regimen	
5-Fluorouracil	90 (73)
Capecitabine	33 (27)
Maintenance chemotherapy	
Yes	113 (92)
No	10 (8)

*Distance from anal verge.

Change of PD-L1, $CD8^+$ and $PD\text{-}1^+$ TILs before and after CRT

The median H-score at pre- and post-CRT was 0 (range, 0–70) and 100 (range, 0–270), respectively, and the median density of pre- and post-CRT $CD8^+$ TILs was 319.66 (range, 20.76–978.08) and 787.05 cells/mm^2 (range, 101.39–2100.85), respectively. PD-1 staining intensity at initial biopsy was scanty, but increased in post-CRT surgical tissues with the median density value of 2.61 cells/mm^2 (range, 0–27.53) (Figure 14).

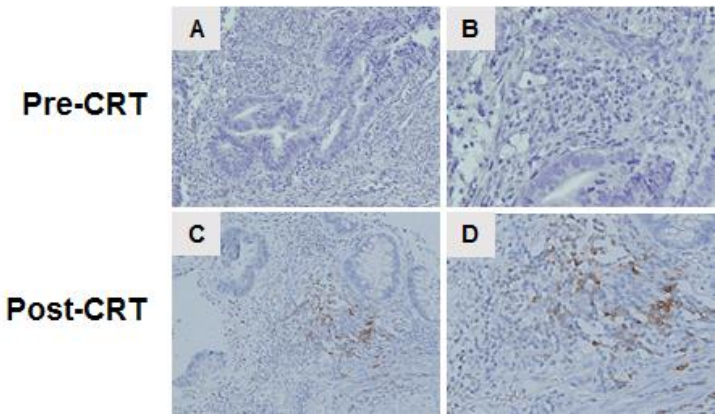

Figure 14. Immunohistochemistry of PD-1 expression at (A, B) pre- and (C, D) post-CRT status (x200 for A and C, and x400 for B and D, respectively).

Each of the median values was used as a cutoff stratifying high or low expression level before and after CRT. Figure 15 shows the representative IHC slide views of PD-L1 and CD8. The scatter dot and before-and-after correspondence plots indicate increased PD-L1 expression after CRT ($P < .001$), and the density of $CD8^+$ TILs

was also significantly increased ($P < .001$) (Figure 16). Figure 17 shows the two representative cases with post-CRT increases of the PD-L1 expression and density of $CD8^+$ TILs. The post-CRT change in the level of $CD8^+$ TILs for each patient was calculated from the formula, $\Delta CD8^+$ TILs = density of post-CRT - pre-CRT $CD8^+$ TILs. Patients with a sustained high PD-L1 level both with pre- and post-CRT status (high-to-high) showed significantly lower $\Delta CD8^+$ TILs than the others ($P = .020$) (Figure 18).

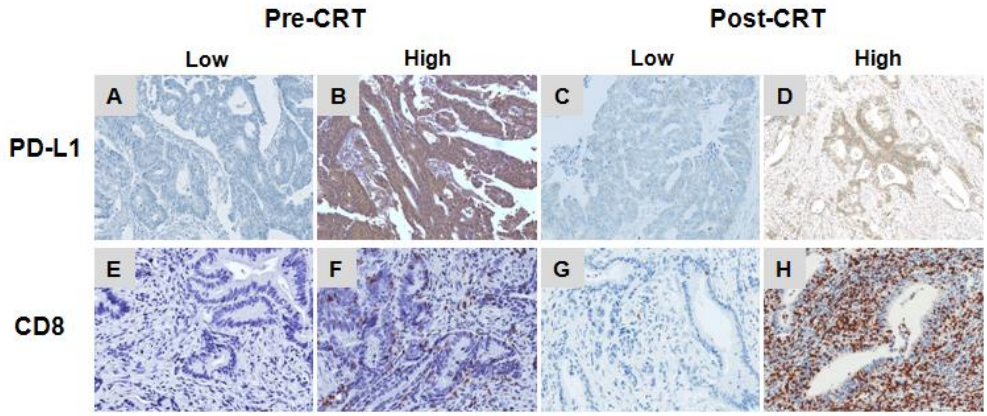

Figure 15. Representative slide views of pre-CRT (A) low and (B) high and post-CRT (C) low and (D) high PD-L1 expressions (*upper panel*) (x200). Pre-CRT (E) low and (F) high and post-CRT (G) low and (H) high density of $CD8^+$ TILs (*lower panel*) (x200).

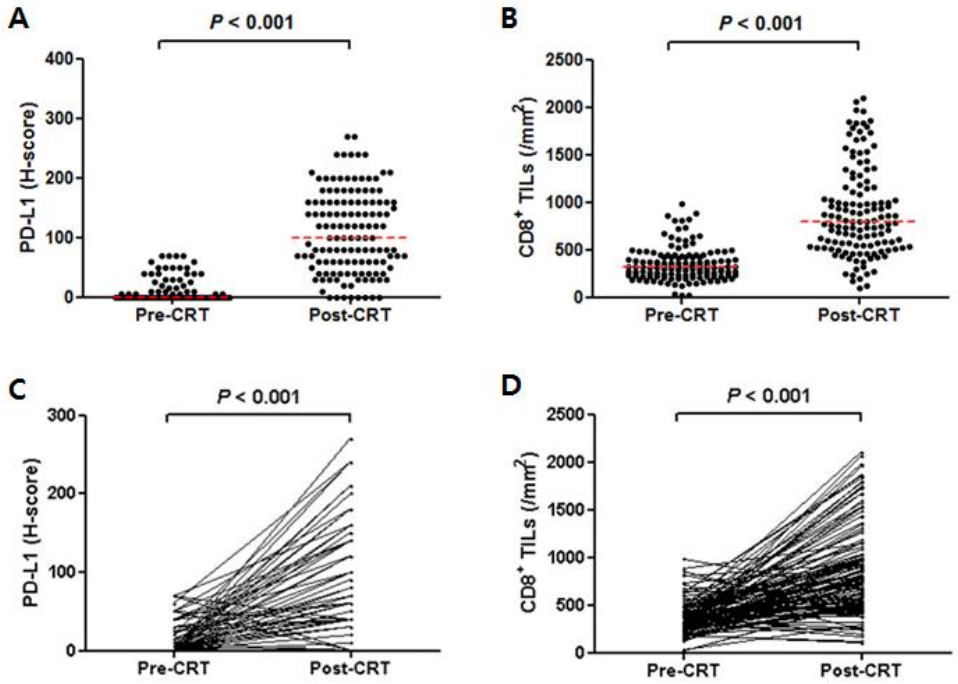

Figure 16. Increased PD-L1 expression and density of $CD8^+$ TILs after CRT. Scatter dot and correspondence plots of (A, C) PD-L1 H-score and (B, D) $CD8^+$ TILs level, respectively.

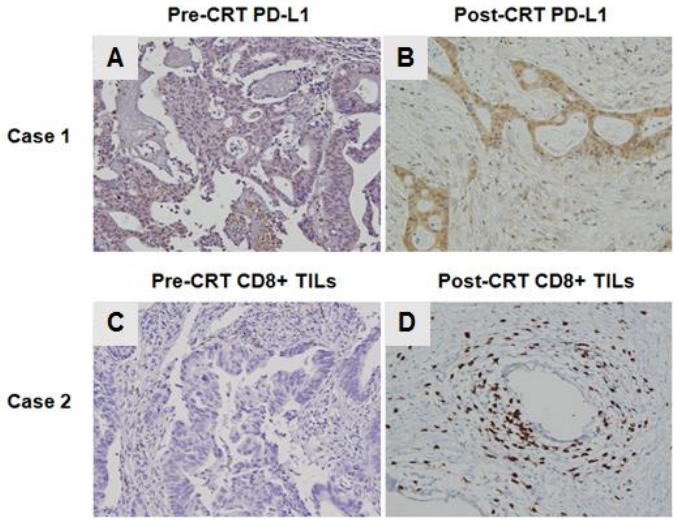

Figure 17. Representative slide views of two cases with CRT-induced increases in the levels of (A, B) PD-L1 and (C, D) $CD8^+$ TILs, respectively (x200).

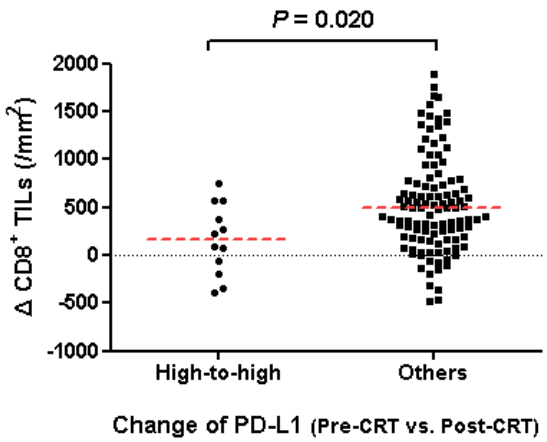

Figure 18. Pre- and post-CRT difference of the density of $CD8^+$ TILs according to the alteration of PD-L1 expression level, high-to-high vs. others. *Red* dotted lines indicate the median values.

Table 2 and 3 represent the association between clinicopathologic characteristics and the expression level of PD-L1 and $CD8^+$ TILs, respectively. Tumor location ≥ 6cm from the anal verge was associated with higher pre-CRT PD-L1 expression and post-CRT $CD8^+$ TILs density (P = .035 for both). Women showed significantly higher density of post-CRT $CD8^+$ TILs (P = .013). Otherwise, there was no statistical significance.

Table 2. Associations between patient characteristics and the expression level of PD-L1 before and after CRT

Variables	N	Pre-CRT [N (%)]		*P*	Post-CRT [N (%)]		*P*
		Low (N=88)	High (N=35)		Low (N=66)	High (N=57)	
Age (years)							
<62	60	46 (52)	14 (40)	.219	32 (48)	28 (49)	.944
≥62	63	42 (48)	21 (60)		34 (52)	29 (51)	
Sex							
Male	86	62 (70)	24 (69)	.837	47 (71)	39 (68)	.736
Female	37	26 (30)	11 (31)		19 (29)	18 (32)	
Tumor location*							
< 6cm	71	56 (64)	15 (43)	.035	43 (65)	28 (49)	.073
≥ 6cm	52	32 (36)	20 (57)		23 (35)	29 (51)	
Tumor grade (biopsy)							
Well differentiated	18	13 (15)	5 (14)	.945	11 (17)	7 (12)	.493
Moderately/Poorly differentiated	105	75 (85)	30 (86)		55 (83)	50 (88)	
cT stage							
T2-3	113	81 (92)	32 (91)	.910	62 (94)	51 (89)	.511
T4	10	7 (8)	3 (9)		4 (6)	6 (11)	
cN stage							
N0	17	15 (17)	2 (6)	.148	10 (15)	7 (12)	.645
N1-2	106	73 (83)	33 (94)		56 (85)	50 (88)	
Tumor grade (surgical)							
Well differentiated	9	8 (9)	1 (3)	.443	6 (9)	3 (5)	.502
Moderately/Poorly differentiated	114	80 (91)	34 (97)		60 (91)	54 (95)	
pT stage							

T1	18	11 (13)	7 (20)	.394	11 (17)	7 (12)	.776
T2	41	32 (36)	9 (26)		21 (32)	20 (35)	
T3	64	45 (51)	19 (54)		34 (51)	30 (53)	
pN stage							
N0	92	67 (76)	25 (71)	.587	54 (82)	38 (67)	.054
N1-2	31	21 (24)	10 (29)		12 (18)	19 (33)	
Downstage of T							
Yes	63	46 (52)	17 (49)	.711	35 (53)	28 (49)	.666
No	60	42 (48)	18 (51)		31 (47)	29 (51)	
Downstage of N[§]							
Yes	81	56 (77)	25 (76)	.915	47 (84)	34 (68)	.054
No	25	17 (23)	8 (24)		9 (16)	16 (32)	
Dworak regression grade							
0-1	58	43 (50)	15 (44)	.561	26 (41)	32 (57)	.071
≥ 2	62	43 (50)	19 (56)		38 (59)	24 (43)	
Lymphatic invasion							
No	103	72 (84)	31 (89)	.584	56 (86)	47 (84)	.732
Yes	18	14 (16)	4 (11)		9 (14)	9 (16)	
Vascular invasion							
No	116	83 (96)	33 (94)	.626	64 (98)	52 (93)	.181
Yes	5	3 (4)	2 (6)		1 (2)	4 (7)	
Perineural invasion							
No	107	76 (88)	31 (89)	.975	60 (92)	47 (84)	.151
Yes	14	10 (12)	4 (11)		5 (8)	9 (16)	
Microsatellite instability							
No	91	67 (92)	24 (89)	.699	44 (90)	47 (92)	.738
Yes	9	6 (8)	3 (11)		5 (10)	4 (8)	

*Distance from anal verge.

§cN0 patients were excluded.

Table 3. Associations between patient characteristics and the expression level of $CD8^+$ TILs before and after CRT

Variables	N	Pre-CRT		Post-CRT	
		Median (cells/mm^2)	*P*	Median (cells/mm^2)	*P*
Age (years)					
<62	60	319.66	.752	783.47	.816
≥62	63	320.61		787.05	
Gender					
Men	86	314.87	.133	721.15	.013
Women	37	352.27		935.34	
Tumor location*					
< 6cm	71	321.29	.302	729.60	.035
≥ 6cm	52	313.67		862.04	
Tumor grade (biopsy)					
Well differentiated	18	416.98	.060	625.96	.052
Moderately/Poorly differentiated	105	308.76		844.10	
cT stage					
T2	7	318.31	.291	902.79	.202
T3	106	324.79		765.01	
T4	10	272.53		1222.75	
cN stage					
N0	17	318.31	.512	749.02	.224
N1-2	106	320.48		795.94	
Tumor grade (surgical)					
Well differentiated	9	416.98	.836	625.96	.641
Moderately/Poorly differentiated	114	308.76		844.10	

pT stage					
T1	18	357.83	.187	659.74	.316
T2	41	326.66		888.33	
T3	64	301.15		749.96	
pN stage					
N0	92	322.92	.283	800.56	.284
N1-2	31	304.13		606.32	
Downstage of T					
Yes	63	332.50	.165	854.84	.175
No	60	299.45		732.75	
Downstage of N[§]					
Yes	81	327.14	.400	844.10	.146
No	25	304.13		586.42	
Dworak regression grade					
0-1	58	302.56	.331	780.41	.625
≥ 2	62	327.63		797.79	
Lymphatic invasion					
No	103	328.48	.004	793.17	.382
Yes	18	225.65		551.47	
Vascular invasion					
No	116	320.48	.260	780.41	.649
Yes	5	176.99		915.67	
Perineural invasion					
No	107	329.33	.027	793.17	.296
Yes	14	250.83		585.22	
Microsatellite instability					
No	91	319.66	.559	798.71	.061

Yes	9	380.80	935.34

*Distance from anal verge.

§cN0 patients were excluded.

Survival analysis

The five-year rates of OS and DFI were 83.4% and 79.2%, respectively, with a median follow-up time of 57.4 months (range, 6.2–134.7). By defining a low or high expression level for PD-L1, as well as the density of $CD8^+$ TILs based on the median values, subgroups with low-to-low, low-to-high, high-to-low, and high-to-high alterations before and after CRT could be specified for each of the markers (n = 44, 44, 22, and 13 for PD-L1; n = 33, 29, 29, and 32 for $CD8^+$ TILs, respectively). The high-to-high PD-L1 group exhibited poorer OS, DFI, and DMFI (*P* = .018, .029, and .023, respectively) (Figure 19), and patients with a low-to-low $CD8^+$ TIL density had an inferior DFI, LRFI, and DMFI (*P* = .010, .014, and .025, respectively) (Figure 20). Considering post-CRT density of $PD\text{-}1^+$ TILs, there were no differences in OS, DFI, LRFI, and DMFI between low vs. high expression level (*P* = .927, .472, .799, and .613, respectively).

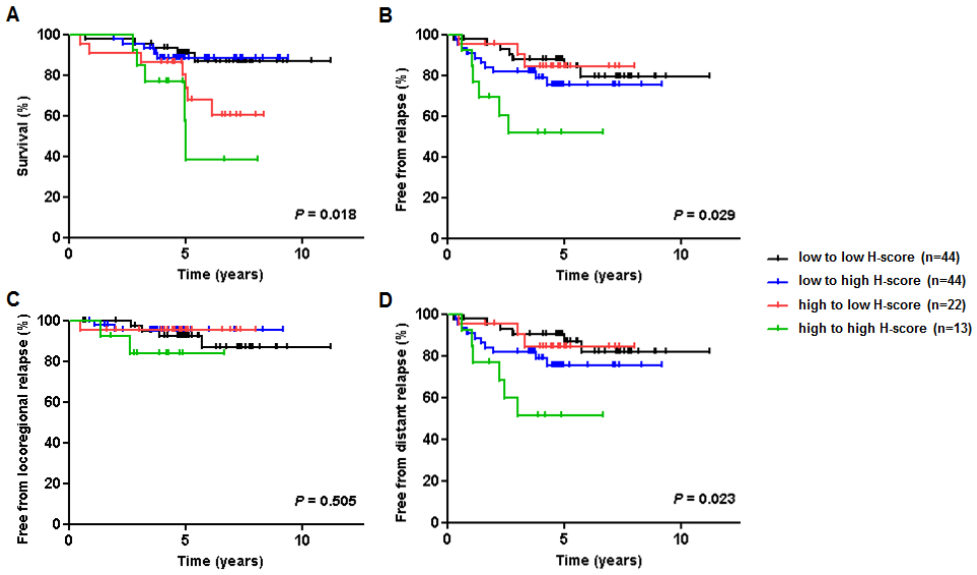

Figure 19. Kaplan-Meier curves according to pre- and post-CRT PD-L1 alteration patterns. (A) Overall survival, (B) disease-free interval, (C) locoregional relapse-free interval, and (D) distant metastasis-free interval.

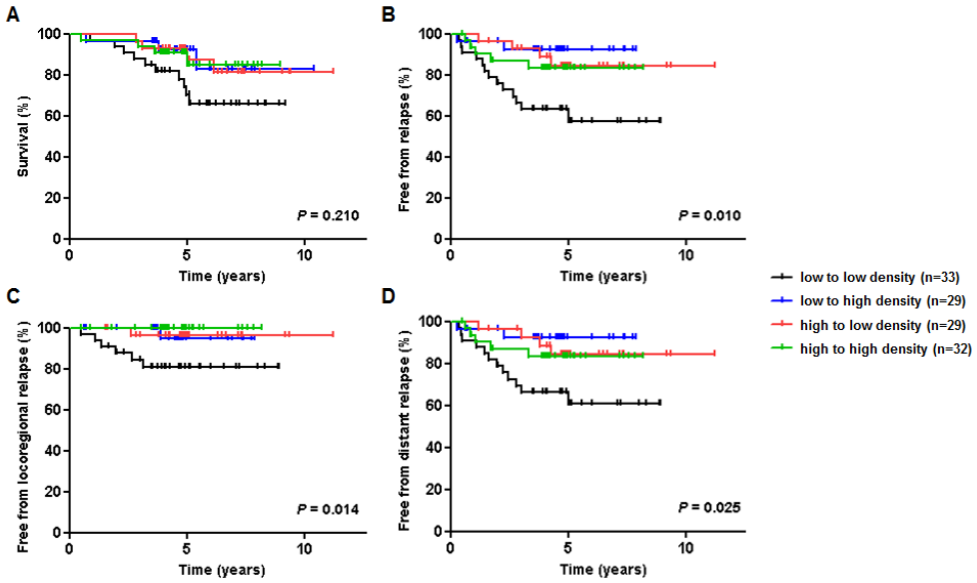

Figure 20. Kaplan-Meier curves according to the CRT-induced alteration of the density of $CD8^+$ TILs. (A) Overall survival, (B) disease-free interval, (C) locoregional relapse-free interval, and (D) distant metastasis-free interval.

Under the assumption that high-to-high PD-L1 expression and low-to-low density of $CD8^+$ TILs are immunologic risk factors, the study population was classified into two groups: one consisting of subjects with neither risk factor and the other consisting of subjects with at least one risk factor. Patients devoid of risk factors had superior OS, DFI, LRFI, and DMFI (P = .020, .002, .017, and .004, respectively) (Figure 21). Subgroup analysis for patients with high-to-high PD-L1 expression revealed differences in the 5-year rates of OS, DFI, LRFI, and DMFI with respect to the relative density of post-CRT $CD8^+$ TILs (low vs. high), as follows: 47.6% vs. 83.3%, 28.6% vs. 83.3%, 71.4% vs. 100%, and 28.6% vs. 83.3%, respectively.

However, none of them was statistically significant, due to limited sample size within each subgroup.

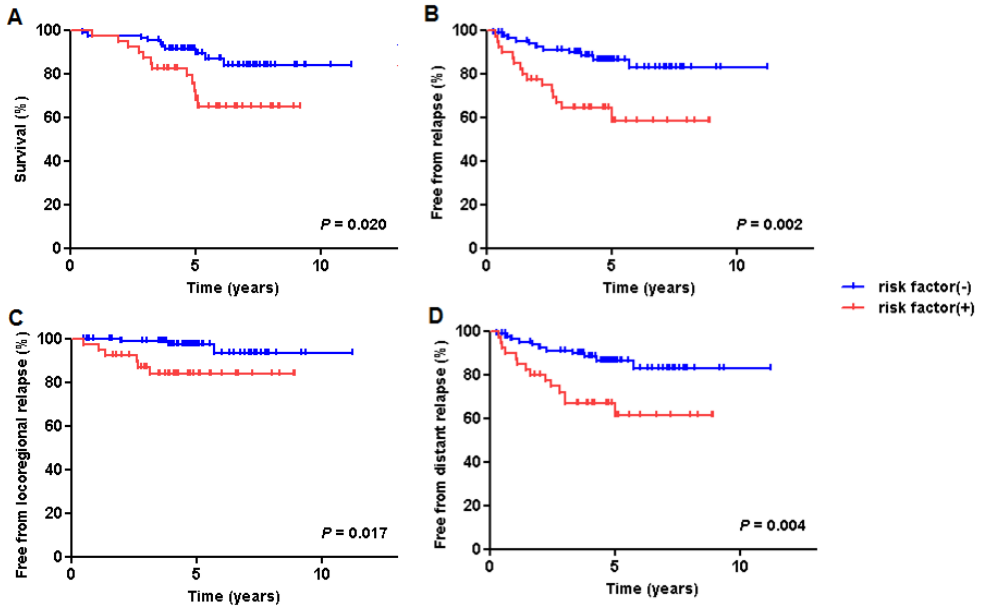

Figure 21. Kaplan-Meier curves according to the existence or non-existence of each of the risk factors: high-to-high PD-L1 level and low-to-low density of $CD8^+$ TILs. (A) Overall survival, (B) disease-free interval, (C) locoregional relapse-free interval, and (D) distant metastasis-free interval.

Table 4 shows the results of multivariate analysis. In OS, two subgroups with high baseline PD-L1 expression level, the high-to-low and high-to-high alterations, showed poor prognosis (hazard ratio [HR] 8.34, 95% confidence interval [CI] 1.85–37.53 and HR 11.03, 95% CI 2.33–52.29, respectively). Due to a relationship

between PD-L1 expression and the density of $CD8^+$ TILs alterations (23), two Cox regression models were utilized to assess prognostic factors of DFI. There was a marginally significant association indicating inferior outcome of tumor recurrence in high-to-high PD-L1 expression (vs. low-to-low PD-L1 expression; HR 3.81, 95% CI 0.96–15.12).

Table 4. Multivariate analysis for overall survival and disease-free interval according to pre- and post-CRT alterations of PD-L1 and $CD8^+$ TILs

Variables*	Overall survival			Disease-free interval (I)			Disease-free interval (II)		
	HR	95% CI	*P*	HR	95% CI	*P*	HR	95% CI	*P*
Sex									
Male	1								
Female	0.46	0.12–1.80	.265						
Tumor location†									
≥ 6cm	1								
< 6cm	3.85	1.24–11.99	.020						
pT stage									
T1-2	1			1			1		
T3	0.31	0.08–1.26	.102	0.71	0.19–2.61	.606	0.74	0.19–2.88	.669
pN stage									
N0	1			1			1		
N1-2	2.42	0.82–7.17	.111	1.36	0.52–3.58	.529	1.13	0.43–3.01	.803
Downstaging									
Yes	1			1			1		
No	6.92	0.96–49.91	.055	4.75	1.09–20.61	.037	3.57	0.73–17.32	.115
Dworak regression grade									
0-1	1			1			1		
2-3	0.44	0.16–1.18	.102	0.53	0.19–1.46	.217	0.34	0.12–0.91	.033
Lymphatic invasion									
No	1			1			1		
Yes	4.46	1.58–12.60	.005	4.16	1.67–10.34	.002	3.04	1.23–7.48	.016
Vascular invasion									

No				1			1		
Yes				3.90	0.94–16.14	.061	5.69	1.24–26.11	.025
Perineural invasion									
No	1			1			1		
Yes	1.39	0.42–4.60	.595	1.63	0.61–4.39	.330	2.06	0.80–5.28	.134
PD-L1 (pre and post)[§]									
Low-to-low	1			1					
Low-to-high	1.21	0.26–5.56	.807	1.23	0.41–3.74	.714			
High-to-low	8.34	1.85–37.53	.006	1.15	2.82–4.71	.844			
High-to-high	11.03	2.33–52.29	.002	3.81	0.96–15.12	.057			
$CD8^+$ TILs (pre and post)[§]									
High-to-high							1		
High-to-low							1.18	0.31–4.46	.812
Low-to-high							0.31	0.06–1.70	.177
Low-to-low							1.53	0.51–4.55	.447

[*]Clinico-pathological variables with *P*-values <0.05 in univariate analysis were included.

[†]Distance from anal verge.

[§]Cutoff values were determined by the median values at pre- and post-CRT.

DISCUSSION

This study explored the RT-induced alterations of PD-1/PD-L1 immune checkpoint based on the CT26 murine tumor model and human rectal cancer tissues. When mouse tumors were irradiated with single ablative and fractionated dose regimen, PD-L1 expression on CT26 tumor cells was highest at the post-RT early phase of descending tumor volume, but abruptly decreased through the "Nadir" and "Regrowth" phases. With a significant increase of $CD8^+$ T cell population, PD-1 expression level on $CD8^+$ T cells was significantly elevated after RT, but not on $CD4^+$ T cells. In rectal cancer patients treated with preoperative CRT, the expression level of PD-1/PD-L1 checkpoint and the density of $CD8^+$ TILs markedly increased after the treatment. Classifying the patient population according to alteration profiles of PD-L1 or $CD8^+$ TIL levels, either a high-to-high H-score of PD-L1 or low-to-low density of $CD8^+$ TILs was associated with worse survival outcomes than those of other groups. Multivariate analysis showed a significant association between high baseline PD-L1 expression and poor OS, with the highest risk observed in the high-to-high PD-L1 subgroup.

From our results of murine tumor model and rectal cancer analysis, more prominent tumor-specific immune responses after RT could be expected. Irradiation of tumor tissues up-regulates tumor-associated antigens and death receptors, such as Fas cell surface death receptor, major histocompatibility complex molecules, and other adhesion-related molecules, and this is an important underlying mechanism of

immunogenic tumor cell death (24). In particular, a surge of tumor antigen loading increases inflammatory cytokines and effector T cells, thereby shifting the immunologic equilibrium of the tumor microenvironment (25, 26). However, the immune system functions with a dynamic balance between stimulatory and inhibitory forces, so this up-shift in anti-tumor immunity is a well-known trigger for inhibitory immune checkpoints (1). The simultaneous up-regulation of immune checkpoint activity and cytotoxic $CD8^+$ T cells in both murine and human models is suggestive of this aspect.

There have been several preclinical studies to investigate how RT affects PD-1/PD-L1 activity in tumors. In an initial research by Deng et al (16), the expression level of PD-1/PD-L1 checkpoint molecules was evaluated using TUBO cell line. Three days after 12 Gy-single dose RT, PD-L1 expression on tumor cells increased, whereas PD-1 expression level was not significantly different compared to non-irradiated tumors. The radiation-induced effect on PD-1/PD-L1 molecules has also been explored using CT26 tumor, but the effect was not monitored through the time course after irradiation (17).

In this study, more prolonged tumor growth delay after 15 Gy x 1 fx than 5 Gy x 3 fx is related to differential level of BED. Nevertheless, either single ablative or fractionated RT up-regulated the PD-L1 expression on tumor cells and PD-1 on $CD8^+$ T cells. A landmark preclinical study using murine melanoma cells also stated that single dose RT of 20 Gy x 1 fx dramatically increased T-cell priming in a $CD8^+$

T cell-dependent fashion (27). However, tumors irradiated with 5 Gy x 4 fx rapidly relapsed, which was analogous to another mouse model of CD8-depleted 20 Gy x 1 fx. The most important factors for these contradictory results might be differences in intrinsic biologic character of tumor cells and radiation-induced tumor cell-killing effect. The B16 melanoma cell line is characterized to be immunogenic and relatively resistant to irradiation (28). Additionally, the fractionated RT regimen of 5 Gy x 4 fx was delivered over 2 weeks, not for 4 consecutive days, suggesting higher potential of damage repair process. In a recent study by Sato et al, depletion of BRCA2 or Ku80 up-regulated PD-L1 expression, highlighting the regulatory role of double-strand break repair in the immunologic tumor microenvironment (29). Therefore, the aforementioned results indicating little immunologic impact of fractionated irradiation need to be interpreted with caution.

However, the RT-induced immediate increase and subsequent decrease of PD-L1 expression within a few days were remarkable, whereas the high-level PD-1-positivity on $CD8^+$ T cells was maintained over the "Nadir" and "Regrowth" phase. This discordance in altered profile of PD-1 and PD-L1 might be because of differential induction of expression as a receptor and ligand, respectively, and this aspect suggests that the receptor-ligand binding activity and related cascade responses would be higher during the early response of RT than a later time. Thus, our results highlight the need of concurrent combination of RT and PD-1/PD-L1 blockade to obtain therapeutic effect to a larger extent.

Several previous syngeneic mouse tumor models have been used to evaluate synergistic effect of combinatory treatment of PD-L1 blockade and irradiation. When CT26 tumors were treated with anti-PD-L1 inhibitor and RT (2 Gy x 5 fx) together (17), the degree of anti-cancer effect was greater and more long-lasting. Three different combinatory schedules were compared, and combining PD-L1 blockade at the first day of RT concurrently resulted in greater tumor-cell killing. Our study of tracking PD-1/PD-L1 activity through the post-RT time course supports the superiority of concurrent initiation of the combinatory treatment, rather than other sequential methods.

Nevertheless, the results from animals cannot be directly extrapolated to clinics. Most of the immunocompetent tumor models were based on subcutaneous tumor tissues. Subcutaneous tumors represent a relatively hypoxic tumor microenvironment compared to that of orthotopic organ sites (30). Considering the potential relationship between oxygen concentration and PD-1/PD-L1 activity, more elevated PD-L1 expression level under hypoxic status has been demonstrated (31). Although preclinical data from mouse models are needed for developing immunotherapy, whether the murine immune system can explain the tumor microenvironment of human cancers is not clear (32). From this study consisting of both murine colon carcinoma model and human rectal cancer tissues, we could obtain comprehensive data of the RT-induced effects on PD-1/PD-L1 axis.

Until recently, there have been a few IHC-based investigations to evaluate the impact of cytotoxic anti-cancer treatments on PD-L1 expression and $CD8^+$ TIL levels (33-37). Similar to our results, a recent study reported up-regulated PD-L1 expression after CRT for rectal cancer (33). However, pre- and post-CRT IHC results were matched and compared only in a small number of patients (n = 63), and there was no further information on TILs in the tumor microenvironment. There was a paired analysis of $CD8^+$ TILs (n = 93), but PD-L1 expression levels were not evaluated (34). Other studies did not assess the potential prognostic significance of CRT-induced alterations in immunologic biomarkers (35-37). Ironically, some previous studies reported a statistically significant and better prognosis in patients with higher PD-L1 expression (33, 38). These contradictory results might be due to inherent confounding factors, such as various kinds of antibodies, inconsistent cutoff values, assay conditions, tumor heterogeneity, and dynamic immune responses. Nevertheless, the prognostic impact of checkpoint molecules has been announced, which suggests that immune checkpoints are clinically relevant in human cancers. Since this study is the largest paired IHC analysis of PD-L1 expression and density of $CD8^+$ TILs to date, it is able to offer useful clinical and prognostic information.

Approximately 15% of colorectal cancer cases are diagnosed as MSI-L or MSI-H status. In contrast to MSS status, MSI tumors inflict a higher mutational load with an elevated level of tumor-specific neo-antigens (38, 39). In this study, the different

MSI statuses did not have significant relationships with PD-L1 expression, pre- and post-CRT, and the density of $CD8^+$ TILs at pre-CRT, but MSI-H or MSI-L tumors had higher numbers of $CD8^+$ TILs at post-CRT with a marginal significance. This lack of statistical significance might be attributable to a relatively low incidence of MSI-H in a study population with only rectal tumors, not proximal or mid-colon cancer (40), as well as incomplete MSI information for a part of the patients. Nevertheless, the CRT-induced immunologic shift might be helpful in expanding the indication and potential applicability of checkpoint inhibitors, even in MSS colorectal tumors. However, further mechanistic investigations are needed.

Regarding clinicopathologic factors in relation to the density of $CD8^+$ TILs, women patients showed a higher level of post-CRT $CD8^+$ TILs. The impact of gender difference on tumor immunity has not been much studied yet, but this point of view has been discussed recently (41, 42). Wesa et al. observed higher frequencies of tumor-associated antigen-specific T cells in female as compared to male patients in melanoma (41). The gender difference might suggest the potential relationships between tumor immunity and hormonal or endocrine status (43, 44). However, in contrast to melanoma, little knowledge has been known in colorectal cancer. Although the gender factor was not associated with differential OS in multivariate analysis in this study, a large-scale population-based analysis of rectal cancer suggested better prognosis in women than men (45). Considering the

potential effects of gender on tumor-specific immune responses, further studies will provide useful information.

Although the high-to-high PD-L1 group did not show a significant difference in LRFI, low-to-low $CD8^+$ TIL level was associated with higher locoregional tumor recurrence. This conflicting result might be explained by the differential biologic role of $CD8^+$ TILs and PD-L1-expressing tumor cells. The $CD8^+$ TILs are the main aggressors involved in killing tumor cells, but PD-1/PD-L1 is one of the immune checkpoints underlying immunologic evasion of tumors (6). In regard to functional relationships among the immune checkpoints (46, 47), we suggest that more comprehensive analysis with other kinds of immune checkpoints would provide additional information.

In recent years, post-treatment failures have also been addressed when treating patients with PD-1/PD-L1 checkpoint inhibitors (48, 49). In turn, potential combinatory strategies using PD-1/PD-L1-inhibiting drugs and other modalities, such as chemotherapy, RT, and CRT, have been proposed to enhance the long-term anti-tumor effects of checkpoint inhibitors (18-20). Cytotoxic treatment with CRT can increase the loading of tumor antigens, their related receptor molecules, and danger-related signal molecules, followed by cascading immune responses (50). Our results indicate that CRT-induced increases in $CD8^+$ TIL density support the principle of an immunologic shift via interferon gamma release. In response to the up-regulation of anti-cancer immunity, PD-L1 expression on tumor cells may be

correspondingly elevated (51). The elevated number of $CD8^+$ TILs would enhance the degree of anti-tumor immune responses (17, 52), whereas pre-existing $CD8^+$ T cells are also required to obtain therapeutic efficacy of anti-PD-1/PD-L1 inhibitors (51). Therefore, this study provides initial insights into the feasibility of such combinatory strategies.

It should be noted, though, that our results are incomplete. PD-L1 expression on infiltrating immune cells could not be assessed in the human cancer specimens, and we evaluated membranous staining intensity of PD-L1 on tumor cells. Kinds of primary tumor tissues, selection of antibody, and assay conditions can affect the staining patterns of each specimen. Although there have been a variety of antibodies for the IHC of PD-L1, some controversies have existed in regard to the standard staining results and antibody validation (53). Given that PD-L1 expression on tumor cells plays a critical role in suppressing T cell responses, and is useful for predicting responses to PD-L1 blockade treatment (54), this study focused on membranous staining results of PD-L1 on tumor cells. Time-matched comparisons between irradiated and non-irradiated mouse tumors might provide useful information, but rapidly growing tumor burden without any treatment and the potential of a consequent ethical problem restricted further analysis. Since the IHC of rectal cancer tissues was retrospectively reviewed in the era of CRT, not RT alone, combined chemotherapeutic effect needs to be considered together in human data.

Our matched analysis of PD-1/PD-L1 axis at pre- and post-irradiation status highlights the immunologic impact of the cytotoxic treatment on the immune checkpoint activity and demonstrates its prognostic associations in clinics. The RT-induced immunologic shift resulted in a sharp increase of PD-L1 expression intensity on tumor cells and PD-1-positive proportions of $CD8^+$ T cell subset. However, PD-L1 expression subsequently decreased within a few days from the time point of maximum, suggesting the need of considering concurrent combinatory strategy of PD-1/PD-L1 blockade and RT. A strong prognostic impact of baseline PD-L1 expression was observed, with the highest risk of deaths observed in the high-to-high PD-L1 alteration group. This comprehensive analysis of syngeneic mouse tumor model and patients' data would provide useful knowledge to optimize the combinatory treatment of PD-L1 blockade and RT in colorectal cancer. Further mechanistic studies are needed to elucidate functional role of RT in tumor immunity.

REFERENCES

1. Chen L, Flies DB. Molecular mechanisms of T cell co-stimulation and co-inhibition. Nat Rev Immunol. 2013;13(4):227-42.
2. Lim S, Phillips JB, Madeira da Silva L, Zhou M, Fodstad O, Owen LB, et al. Interplay between Immune Checkpoint Proteins and Cellular Metabolism. Cancer Res. 2017;77(6):1245-9.
3. Keir ME, Butte MJ, Freeman GJ, Sharpe AH. PD-1 and its ligands in tolerance and immunity. Annu Rev Immunol. 2008;26:677-704.
4. Zitvogel L, Kroemer G. Targeting PD-1/PD-L1 interactions for cancer immunotherapy. Oncoimmunology. 2012;1(8):1223-5.
5. Chen L, Han X. Anti-PD-1/PD-L1 therapy of human cancer: past, present, and future. J Clin Invest. 2015;125(9):3384-91.
6. Pardoll DM. The blockade of immune checkpoints in cancer immunotherapy. Nat Rev Cancer. 2012;12(4):252-64.
7. Siegel RL, Miller KD, Jemal A. Cancer Statistics, 2017. CA Cancer J Clin. 2017;67(1):7-30.
8. Yeo SG, Kim MJ, Kim DY, Chang HJ, Kim MJ, Baek JY, et al. Patterns of failure in patients with locally advanced rectal cancer receiving pre-operative or post-operative chemoradiotherapy. Radiat Oncol. 2013;8:114.
9. Toh JW, de Souza P, Lim SH, Singh P, Chua W, Ng W, et al. The Potential Value of Immunotherapy in Colorectal Cancers: Review of the Evidence for

Programmed Death-1 Inhibitor Therapy. Clin Colorectal Cancer. 2016;15(4):285-91.

10. Le DT, Uram JN, Wang H, Bartlett BR, Kemberling H, Eyring AD, et al. PD-1 Blockade in Tumors with Mismatch-Repair Deficiency. N Engl J Med. 2015;372(26):2509-20.

11. Brahmer JR, Tykodi SS, Chow LQ, Hwu WJ, Topalian SL, Hwu P, et al. Safety and activity of anti-PD-L1 antibody in patients with advanced cancer. N Engl J Med. 2012;366(26):2455-65.

12. Zitvogel L, Apetoh L, Ghiringhelli F, Kroemer G. Immunological aspects of cancer chemotherapy. Nat Rev Immunol. 2008;8(1):59-73.

13. Formenti SC, Demaria S. Systemic effects of local radiotherapy. Lancet Oncol. 2009;10(7):718-26.

14. Schmidt MA, Fortsch C, Schmidt M, Rau TT, Fietkau R, Distel LV. Circulating regulatory T cells of cancer patients receiving radiochemotherapy may be useful to individualize cancer treatment. Radiother Oncol. 2012;104(1):131-8.

15. Schaue D, Comin-Anduix B, Ribas A, Zhang L, Goodglick L, Sayre JW, et al. T-cell responses to survivin in cancer patients undergoing radiation therapy. Clin Cancer Res. 2008;14(15):4883-90.

16. Deng L, Liang H, Burnette B, Beckett M, Darga T, Weichselbaum RR, et al. Irradiation and anti-PD-L1 treatment synergistically promote antitumor immunity in mice. J Clin Invest. 2014;124(2):687-95.

17. Dovedi SJ, Adlard AL, Lipowska-Bhalla G, McKenna C, Jones S, Cheadle EJ, et al. Acquired resistance to fractionated radiotherapy can be overcome by concurrent PD-L1 blockade. Cancer Res. 2014;74(19):5458-68.

18. Reck M, Rodriguez-Abreu D, Robinson AG, Hui R, Csoszi T, Fulop A, et al. Pembrolizumab versus Chemotherapy for PD-L1-Positive Non-Small-Cell Lung Cancer. N Engl J Med. 2016;375(19):1823-33.

19. Katz MHG, Bauer TW, Varadhachary GR, Petroni GR, Bullock T, Slingluff CL, et al. A randomized multicenter phase Ib/II study to assess the safety and the immunological effect of chemoradiation therapy (CRT) in combination with pembrolizumab (anti-PD1) to CRT alone in patients with resectable or borderline resectable pancreatic cancer. Journal of Clinical Oncology. 2015;33(suppl):abstr TPS3098.

20. Antonia SJ, Brahmer JR, Gettinger S, Chow LQ, Juergens R, Shepherd FA, et al. Nivolumab (Anti-PD-1; BMS-936558, ONO-4538) in Combination With Platinum-Based Doublet Chemotherapy (PT-DC) in Advanced Non-Small Cell Lung Cancer (NSCLC). International Journal of Radiation Oncology • Biology • Physics. 2014;90(5):S2.

21. Liu CY, Liao HF, Wang TE, Lin SC, Shih SC, Chang WH, et al. Etoposide sensitizes CT26 colorectal adenocarcinoma to radiation therapy in BALB/c mice. World J Gastroenterol. 2005;11(31):4895-8.

22. Dworak O, Keilholz L, Hoffmann A. Pathological features of rectal cancer after

preoperative radiochemotherapy. Int J Colorectal Dis. 1997;12(1):19-23.

23. Van Steen K, Curran D, Kramer J, Molenberghs G, Van Vreckem A, Bottomley A, et al. Multicollinearity in prognostic factor analyses using the EORTC QLQ-C30: identification and impact on model selection. Stat Med. 2002;21(24):3865-84.

24. Jochems C, Schlom J. Tumor-infiltrating immune cells and prognosis: the potential link between conventional cancer therapy and immunity. Exp Biol Med (Maywood). 2011;236(5):567-79.

25. Strome SE, Voss S, Wilcox R, Wakefield TL, Tamada K, Flies D, et al. Strategies for antigen loading of dendritic cells to enhance the antitumor immune response. Cancer Res. 2002;62(6):1884-9.

26. Bracci L, Schiavoni G, Sistigu A, Belardelli F. Immune-based mechanisms of cytotoxic chemotherapy: implications for the design of novel and rationale-based combined treatments against cancer. Cell Death Differ. 2014;21(1):15-25.

27. Lee Y, Auh SL, Wang Y, Burnette B, Wang Y, Meng Y, et al. Therapeutic effects of ablative radiation on local tumor require CD8+ T cells: changing strategies for cancer treatment. Blood. 2009;114(3):589-95.

28. Overwijk WW, Restifo NP. B16 as a mouse model for human melanoma. Curr Protoc Immunol. 2001;Chapter 20:Unit 20.1.

29. Sato H, Niimi A, Yasuhara T. DNA double-strand break repair pathway regulates PD-L1 expression in cancer cells. 2017;8(1):1751.

30. Graves EE, Vilalta M, Cecic IK, Erler JT, Tran PT, Felsher D, et al. Hypoxia in models of lung cancer: implications for targeted therapeutics. Clin Cancer Res. 2010;16(19):4843-52.

31. Noman MZ, Desantis G, Janji B, Hasmim M, Karray S, Dessen P, et al. PD-L1 is a novel direct target of HIF-1alpha, and its blockade under hypoxia enhanced MDSC-mediated T cell activation. J Exp Med. 2014;211(5):781-90.

32. Budhu S, Wolchok J, Merghoub T. The importance of animal models in tumor immunity and immunotherapy. Curr Opin Genet Dev. 2014;24:46-51.

33. Hecht M, Buttner-Herold M, Erlenbach-Wunsch K, Haderlein M, Croner R, Grutzmann R, et al. PD-L1 is upregulated by radiochemotherapy in rectal adenocarcinoma patients and associated with a favourable prognosis. Eur J Cancer. 2016;65:52-60.

34. Shinto E, Hase K, Hashiguchi Y, Sekizawa A, Ueno H, Shikina A, et al. CD8+ and FOXP3+ tumor-infiltrating T cells before and after chemoradiotherapy for rectal cancer. Ann Surg Oncol. 2014;21 Suppl 3:S414-21.

35. Lim SH, Hong M, Ahn S, Choi YL, Kim KM, Oh D, et al. Changes in tumour expression of programmed death-ligand 1 after neoadjuvant concurrent chemoradiotherapy in patients with squamous oesophageal cancer. Eur J Cancer. 2016;52:1-9.

36. Saigusa S, Toiyama Y, Tanaka K, Inoue Y, Mori K, Ide S, et al. Implication of programmed cell death ligand 1 expression in tumor recurrence and prognosis in

rectal cancer with neoadjuvant chemoradiotherapy. Int J Clin Oncol. 2016;21(5):946-52.

37. Teng F, Meng X, Kong L, Mu D, Zhu H, Liu S, et al. Tumor-infiltrating lymphocytes, forkhead box P3, programmed death ligand-1, and cytotoxic T lymphocyte-associated antigen-4 expressions before and after neoadjuvant chemoradiation in rectal cancer. Transl Res. 2015;166(6):721-32.e1.

38. Droeser RA, Hirt C, Viehl CT, Frey DM, Nebiker C, Huber X, et al. Clinical impact of programmed cell death ligand 1 expression in colorectal cancer. Eur J Cancer. 2013;49(9):2233-42.

39. Xiao Y, Freeman GJ. The microsatellite instable subset of colorectal cancer is a particularly good candidate for checkpoint blockade immunotherapy. Cancer Discov. 2015;5(1):16-8.

40. Phipps AI, Lindor NM, Jenkins MA, Baron JA, Win AK, Gallinger S, et al. Colon and rectal cancer survival by tumor location and microsatellite instability: the Colon Cancer Family Registry. Dis Colon Rectum. 2013;56(8):937-44.

41. Wesa AK, Mandic M, Taylor JL, Moschos S, Kirkwood JM, Kwok WW, et al. Circulating Type-1 Anti-Tumor CD4(+) T Cells are Preferentially Pro-Apoptotic in Cancer Patients. Front Oncol. 2014;4:266.

42. Ramirez AG, Wages NA, Hu Y, Smolkin ME, Slingluff CL, Jr. Defining the effects of age and gender on immune response and outcomes to melanoma vaccination: a retrospective analysis of a single-institution clinical trials'

experience. Cancer Immunol Immunother. 2015;64(12):1531-9.

43. Mervic L. Time course and pattern of metastasis of cutaneous melanoma differ between men and women. PLoS One. 2012;7(3):e32955.

44. Kemeny MM, Busch E, Stewart AK, Menck HR. Superior survival of young women with malignant melanoma. Am J Surg. 1998;175(6):437-44; discussion 44-5.

45. Lee YC, Lee YL, Chuang JP, Lee JC. Differences in survival between colon and rectal cancer from SEER data. PLoS One. 2013;8(11):e78709.

46. Llosa NJ, Cruise M, Tam A, Wicks EC, Hechenbleikner EM, Taube JM, et al. The vigorous immune microenvironment of microsatellite instable colon cancer is balanced by multiple counter-inhibitory checkpoints. Cancer Discov. 2015;5(1):43-51.

47. Schlosser HA, Drebber U, Kloth M, Thelen M, Rothschild SI, Haase S, et al. Immune checkpoints programmed death 1 ligand 1 and cytotoxic T lymphocyte associated molecule 4 in gastric adenocarcinoma. Oncoimmunology. 2016;5(5):e1100789.

48. Bowyer S, Prithviraj P, Lorigan P, Larkin J, McArthur G, Atkinson V, et al. Efficacy and toxicity of treatment with the anti-CTLA-4 antibody ipilimumab in patients with metastatic melanoma after prior anti-PD-1 therapy. Br J Cancer. 2016;114(10):1084-9.

49. Kirchberger MC, Hauschild A, Schuler G, Heinzerling L. Combined low-dose

ipilimumab and pembrolizumab after sequential ipilimumab and pembrolizumab failure in advanced melanoma. Eur J Cancer. 2016;65:182-4.

50. Kaur P, Asea A. Radiation-induced effects and the immune system in cancer. Front Oncol. 2012;2:191.

51. Tumeh PC, Harview CL, Yearley JH, Shintaku IP, Taylor EJ, Robert L, et al. PD-1 blockade induces responses by inhibiting adaptive immune resistance. Nature. 2014;515(7528):568-71.

52. Dovedi SJ, Illidge TM. The antitumor immune response generated by fractionated radiation therapy may be limited by tumor cell adaptive resistance and can be circumvented by PD-L1 blockade. Oncoimmunology. 2015;4(7):e1016709.

53. Caldwell C, Jr., Johnson CE, Balaji VN, Balaji GA. Identification and Validation of a PD-L1 Binding Peptide for Determination of PDL1 Expression in Tumors. 2017;7(1):13682.

54. Juneja VR, McGuire KA, Manguso RT, LaFleur MW, Collins N, Haining WN, et al. PD-L1 on tumor cells is sufficient for immune evasion in immunogenic tumors and inhibits CD8 T cell cytotoxicity. J Exp Med. 2017;214(4):895-904.

국문 초록

서론: 최근 면역 치료의 발전으로 PD-1/PD-L1 억제가 암 치료의 새로운 표적으로 소개되었지만, 대부분 재발성이나 전이성 암에 국한하여 활용되어 왔다. 방사선 치료는 주된 암 치료의 한 부분으로서 직접적으로 세포를 죽이는데, 이를 통해 항종양 면역 반응이 상향 조절된다. 하지만 방사선 치료의 PD-1/PD-L1 면역 관문에 대한 면역학적 영향에 대해서는 현재까지 많이 논의되지 않았다. 이 연구는 마우스 대장암 종양 모델과 수술 전 항암방사선 치료를 받은 직장암 환자 정보를 기반으로 방사선 치료에 의해 유도되는 PD-1/PD-L1 면역 관문 분자들의 발현 변화에 대해 알아보았다.

방법: CT26 대장암 세포주를 BALB/c 마우스 우측 뒷다리에 피하 주입했다. 15 Gy x 1 fx 또는 5 Gy x 3 fx 의 방사선 조사 후 얻어진 종양 용적 변화 곡선 추세를 기반으로, 마우스 종양을 총 4 가지의 개별 시점에서 외과적으로 절제했다. “방사선 치료 전 (Pre-RT)”은 방사선 치료 시작 직전 방사선 조사가 이뤄지지 않은 상태를 의미, “초기 (Early)”은 방사선 치료 반응의 초기 단계, “최저 (Nadir)”는 종양 용적의 최소값을 나타내는 시점, 그리고 “재성장 (Regrowth)”은 방사선 치료 후 종양이 다시 성장하는 시기를 의미한다. 방사선 조사 시작일을 Day 1 으로 정의했을 때, 단일 절제 선량 하에서는 Day 1, 6, 12, 22, 분할 선량 방식 하에서는 Day 1, 6, 10, 20 에 각각의 시점에

해당하는 개별 종양 조직을 얻었다. 종양 세포에서의 PD-L1 발현, 종양 침윤 $CD4^+$ 및 $CD8^+$ T 세포군의 분율, 그리고 $CD4^+$ 및 $CD8^+$ T 세포에서의 PD-1 발현 등을 유세포 분석 방식으로 측정했다. 사람 데이터와 관련하여, 2005 년부터 2012 년에 걸쳐 수술 전 항암방사선 치료 후 수술을 시행 받은 직장암 환자 123 명을 대상으로 항암방사선 치료 전 조직 검사 시 획득한 검체와 이에 대응하는 항암방사선 치료 후 절제된 조직을 활용한 짝지은 분석을 시행했다. 환자들의 임상병리학적 인자 및 생존 결과 데이터와 함께 PD-L1, PD-1, CD8 의 면역조직화학염색을 시행했다.

결과: 마우스 종양 세포에서의 PD-L1 발현은 방사선 치료 종료 후 수일 내에 급격히 증가했으며, 이후 "최저 (Nadir)" 및 "재성장 (Regrowth)" 시기에 가파른 감소를 보였다 (단일 절제 선량 및 분할 선량 별로 각각 $P < .001$ 및 .002). 방사선 치료 효과 기간에 해당하는 "초기 (Early)" 및 "최저 (Nadir)" 시점에서 $CD4^+$ T 세포는 감소했지만 $CD8^+$ T 세포는 증가했다. 이러한 변화 경향은 "재성장 (Regrowth)" 기간에 뒤바뀌었는데, $CD4^+$ T 세포는 다시 증가, $CD8^+$ T 세포는 다시 감소하는 추세를 보였다. 이러한 시점별 차이는 통계적으로 유의했다 (모든 비교에서 $P < .001$). $CD4^+$ T 세포에서의 PD-1 양성률(%)은 시점 별로 유의한 차이가 없었다 (단일 절제 선량 및 분할 선량 별로 각각 $P = .590$ 및 .238). 대조적으로, $CD8^+$ T 세포

에서의 PD-1 양성 비율(%)은 가파르게 증가했고, 이 높은 수준은 “재성장(Regrowth)” 단계까지도 유지되었다 (모든 비교에서 $P < .001$).

직장암의 면역조직화학염색에서는 항암방사선 치료 후 PD-L1 발현 수준과 $CD8^+$ 종양 침윤 림프구 밀도가 증가한 것으로 나타났다 (두 비교에서 $P < .001$). PD-1 의 경우, 항암방사선 치료 전 발현 강도는 매우 미약했으나, 항암방사선 치료 후 눈에 띄게 증가했다. 각 발현도의 중앙값을 기준치로 선정했을 때, 치료 전 후에 걸쳐 지속적으로 높은 PD-L1 발현(높음-높음)을 보이는 것이 치료 후 $CD8^+$ 종양 침윤 림프구 밀도의 보다 적은 증가로 이어졌다 ($P = .020$). 치료 전 후 높은 PD-L1 발현(높음-높음)을 보이는 환자들이 전체 생존율과 무질환 기간에서 더 나쁜 성적을 나타냈으며 (각각 $P = .018$ 및 .029), 치료 전 후 지속적으로 낮은 $CD8^+$ 종양 침윤 림프구 밀도(낮음-낮음)를 보이는 경우에 무질환 기간 성적이 더 나쁜 것으로 관찰되었다. 다변량 분석에서 치료 전 높은 기저 PD-L1 발현을 보이는 두 그룹이 유의하게 좋지 않은 전체 생존율을 보였는데, 치료 전 후 지속적으로 PD-L1 이 발현이 높은(높음-높음) 그룹이 가장 높은 위험도를 나타냈다 (치료 전 후 각각 높고 낮은 PD-L1 발현(높음-낮음)을 보이는 그룹: 위험도 8.34, 95% 신뢰구간 [CI]; 치료 전 후 모두 높은 PD-L1 발현(높음-높음)을 보이는 그룹: 위험도 11.03, 95% 신뢰구간 2.33–52.29).

결론: 본 연구는 방사선 조사에 의해 유도되는 PD-1/PD-L1 면역 관문 활성도와 $CD8^+$ 종양 침윤 림프구 밀도를 증가시키는 방향의 면역학적 변화를 확인했다. 하지만 이러한 변화가 오래 지속되지는 않았고 방사선 치료 효과가 끝난 후에 다시 회복하는 경향을 보였는데, 이는 PD-L1 억제와 방사선 조사를 시간적으로 동시에 병합하는 치료 방침의 필요성을 강조하는 것이라고 볼 수 있다. 이러한 면역 관문 관련 분자들의 발현 변화를 통해 나쁜 예후를 보이는 환자 집단을 확인할 수 있었고, 항암방사선 치료와 면역 관문 억제 병합 치료의 이득이 기대되는 잠정적인 후보 환자군을 제시했다.

* 본 내용의 일부는 미국방사선종양학회지 (International Journal of Radiation Oncology ▪ Biology ▪ Physics. 2017;99(5):1216-24)에 출판되었음.

주요어 : PD-L1, PD-1, CD8, 방사선 치료, 마우스 종양 모델, 직장암, 항암방사선 치료

학 번 : 2014-30918